SAND2019-8679C

Computational Peridynamics

David Littlewood
Sandia National Laboratories

John Foster
University of Texas

Pablo Seleson
Oak Ridge National Laboratory

15th U.S. Nation Congress on Computational Mechanics

July 28th, 2019

Sandia National Laboratories is a multi-mission laboratory managed and operated by National Technology and Engineering Solutions of Sandia, LLC., a wholly owned subsidiary of Honeywell International, Inc., for the U.S. Department of Energy's National Nuclear Security Administration under contract DE-NA0003525.

Short Course
Peridynamic Theory of Solid Mechanics

Outline

- Ingredients of a peridynamics simulation
  - Governing equations
  - Constitutive model, bond failure law
  - Contact model
  - Discretization
  - Time integrator
- Surface effect in peridynamic simulations
- Estimation of the maximum stable time step for dynamic simulations
- Convergence of peridynamic models
- Demonstration of meshfree peridynamics for model analysis
- Modeling damage and failure

Ingredients for computational peridynamics

- Governing equations
  - Continuum form of the balance of linear momentum

$$\rho(\mathbf{x})\ddot{\mathbf{u}}(\mathbf{x},t) = \int_{\mathcal{B}} \left\{ \underline{\mathbf{T}}[\mathbf{x},t]\,\langle \mathbf{x}' - \mathbf{x} \rangle - \underline{\mathbf{T}}'[\mathbf{x}',t]\,\langle \mathbf{x} - \mathbf{x}' \rangle \right\} \mathrm{d}V_{\mathbf{x}'} + \mathbf{b}(\mathbf{x},t)$$

  - Semi-discrete form: meshless discretization of the strong form

$$\rho(\mathbf{x})\ddot{\mathbf{u}}_h(\mathbf{x},t) = \sum_{i=0}^{N} \left\{ \underline{\mathbf{T}}[\mathbf{x},t]\,\langle \mathbf{x}'_i - \mathbf{x} \rangle - \underline{\mathbf{T}}'[\mathbf{x}'_i,t]\,\langle \mathbf{x} - \mathbf{x}'_i \rangle \right\} \Delta V_{\mathbf{x}'_i} + \mathbf{b}(\mathbf{x},t)$$

- Boundary and initial conditions
- Constitutive model
- Bond failure law
- Contact model
- Discretization
- Time integration
  - Explicit
  - Implicit
- Pre- and post-processing

Meshfree peridynamic model of an expanding, fragmenting cylinder

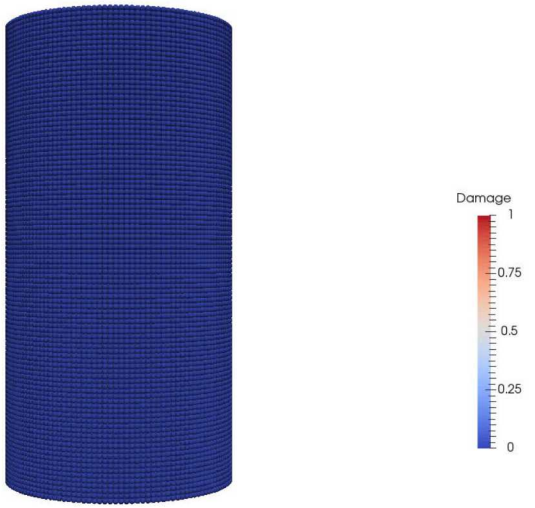

S.A. Silling. Reformulation of elasticity theory for discontinuities and long-range forces. *Journal of the Mechanics and Physics of Solids*, 48:175-209, 2000.

S.A. Silling and E. Askari. A meshfree method based on the peridynamic model of solid mechanics. *Computers and Structures*, 83:1526-1535, 2005.

Model for a peridynamics simulation code

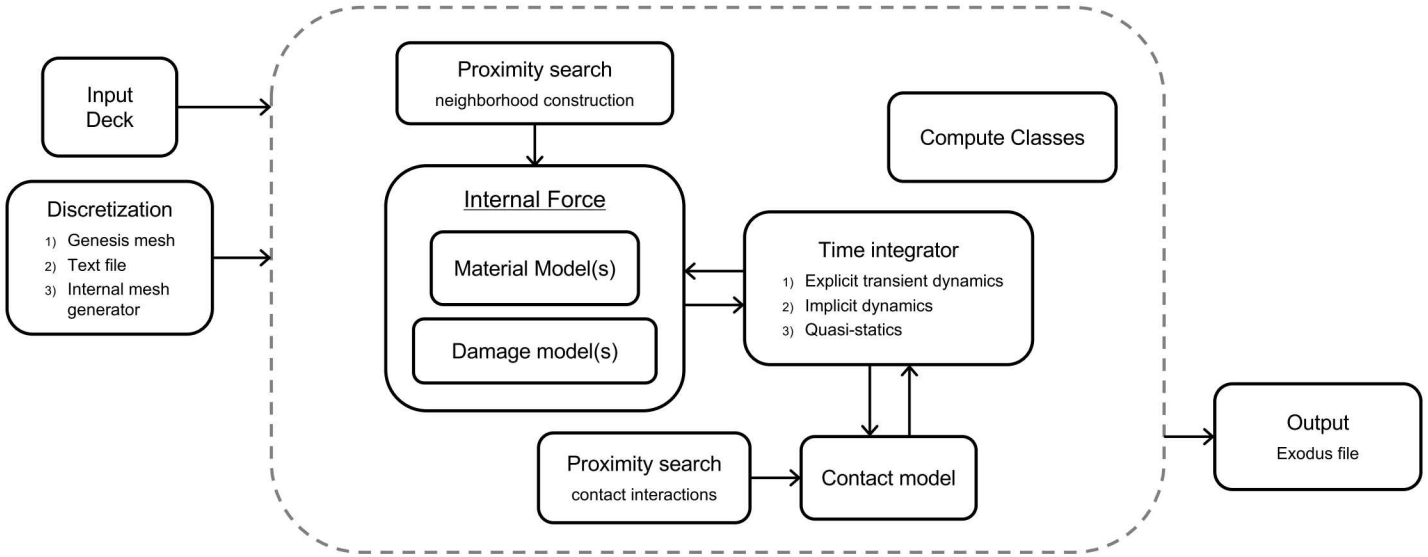

Constitutive models

- Bond-based models
  - Direct pairwise interactions
- State-based models
  - Multi-point interactions
- Correspondence models
  - Wrapper for classic stress-strain models

Example: Linear peridynamic solid [Silling]

- State-based model
- Deformation decomposed into deviatoric and dilatational components

$$\theta = \frac{3}{m}\int_{\mathcal{H}} (\underline{\omega}\,\underline{x})\cdot\underline{e}\,dV \qquad \underline{e}^d = \underline{e} - \frac{\theta\,\underline{x}}{3}$$

- Magnitude of pairwise force density given by

$$\underline{t} = \frac{3k\theta}{m}\,\underline{\omega}\,\underline{\mathrm{x}} + \frac{15\mu}{m}\,\underline{\omega}\,\underline{e}^{\mathrm{d}}$$

S.A. Silling, M. Epton, O. Weckner, J. Xu, and E. Askari, Peridynamic states and constitutive modeling, *Journal of Elasticity*, 88, 2007.

Software implementation of the Linear Peridynamic Solid

Algorithm 1 The initialization routine for a *linear peridynamic solid* material with a Gaussian influence function.

procedure LINEAR PERIDYNAMIC SOLID INITIALIZATION
  ▷ Compute the weighted volume for each node.
  for each node i **do**
    $m_i \leftarrow 0$
    for each node j in neighbor list for node i **do**
      $\boldsymbol{\xi} \leftarrow \mathbf{x}_j - \mathbf{x}_i$
      $\underline{\omega} \leftarrow \exp\left(-\frac{|\boldsymbol{\xi}|^2}{\delta^2}\right)$
      $m_i \leftarrow m_i + \underline{\omega}\,|\boldsymbol{\xi}|^2\,\Delta V_j$
    end for
  end for
end procedure

Algorithm 2 Routine for calculation of the internal force density for a *linear peridynamic solid* material with a Gaussian influence function.

procedure LINEAR PERIDYNAMIC SOLID INTERNAL FORCE
  ▷ Initialize the global force density vector to zero.
  for each node i **do**
    $\mathbf{f}_i \leftarrow 0$
  end for
  ▷ Compute the dilatation for each node.
  for each node i **do**
    $\theta_i \leftarrow 0$
    for each node j in neighbor list for node i **do**
      $\boldsymbol{\xi} \leftarrow \mathbf{x}_j - \mathbf{x}_i$
      $\boldsymbol{\eta} \leftarrow \mathbf{u}_j - \mathbf{u}_i$
      $\underline{\omega} \leftarrow \exp\left(-\frac{|\boldsymbol{\xi}|^2}{\delta^2}\right)$
      $\underline{e} \leftarrow |\boldsymbol{\xi} + \boldsymbol{\eta}| - |\boldsymbol{\xi}|$
      $\theta_i \leftarrow \theta_i + \frac{3}{m_i}\,\underline{\omega}\,|\boldsymbol{\xi}|\,\underline{e}\,\Delta V_j$
    end for
  end for
  ▷ Compute the pairwise contributions to the global force density vector.
  for each node i **do**
    for each node j in neighbor list for node i **do**
      $\boldsymbol{\xi} \leftarrow \mathbf{x}_j - \mathbf{x}_i$
      $\boldsymbol{\eta} \leftarrow \mathbf{u}_j - \mathbf{u}_i$
      $\underline{\omega} \leftarrow \exp\left(-\frac{|\boldsymbol{\xi}|^2}{\delta^2}\right)$
      $\underline{e} \leftarrow |\boldsymbol{\xi} + \boldsymbol{\eta}| - |\boldsymbol{\xi}|$
      $\underline{e}^d \leftarrow \underline{e} - \frac{\theta_i\,|\boldsymbol{\xi}|}{3}$
      $\underline{t} \leftarrow \frac{3}{m_i}\,k\,\theta_i\,\underline{\omega}\,|\boldsymbol{\xi}| + \frac{15\mu}{m_i}\,\underline{\omega}\,\underline{e}^d$
      $\underline{\mathbf{M}} \leftarrow \frac{\boldsymbol{\xi}+\boldsymbol{\eta}}{|\boldsymbol{\xi}+\boldsymbol{\eta}|}$
      $\mathbf{f}_i \leftarrow \mathbf{f}_i + \underline{t}\,\underline{\mathbf{M}}\,\Delta V_j$
      $\mathbf{f}_j \leftarrow \mathbf{f}_j - \underline{t}\,\underline{\mathbf{M}}\,\Delta V_i$
    end for
  end for
end procedure

David J. Littlewood. Roadmap for Peridynamic Software Implementation. SAND Report 2015-9013. Sandia National Laboratories, Albuquerque, NM and Livermore, CA, 2015.

Bond failure law

- Critical stretch [Silling]
  - Brittle failure
  - Critical stretch value determined from the material's energy release rate
- Energy-based approach [Foster]
- Ductile failure models [Silling]

Example: Critical stretch law

- Bond fails irreversibly when critical stretch is exceeded

$$s_{\max} = \frac{y_{\max} - x}{x} \qquad \mathrm{d} = \begin{cases} 0 & \text{if} \quad s_{\max} < s_o \\ 1 & \text{if} \quad s_{\max} \geq s_0 \end{cases}$$

S.A. Silling, M. Epton, O. Weckner, J. Xu, and E. Askari, Peridynamic states and constitutive modeling, *Journal of Elasticity*, 88, 2007.

Software implementation of the Critical Stretch Bond Failure Law

Algorithm 3 Routine for evaluation of the *critical stretch* bond failure law. Bond damage values, d_{ij}, are initialized to zero at the beginning of the simulation and set to a value of one if the bond stretch exceeds the specified critical value.

```
1: procedure CRITICAL STRETCH BOND FAILURE
2:     for each node i do
3:         ▷ Evaluate the stretch of each bond.
4:         for each node j in neighbor list for node i do
5:             ξ ← x_j − x_i
6:             η ← u_j − u_i
7:             s = (|ξ+η| − |ξ|) / |ξ|
8:             ▷ Check the bond stretch against the critical value.
9:             if s ≥ s_o then
10:                d_ij = 1.0
11:            end if
12:        end for
13:    end for
14: end procedure
```

Modeling contact

- Contact algorithms involve two distinct steps:
  - Proximity search
  - Enforcement
- The majority of meshfree peridynamic simulations to date have utilized the short-range force approach of Silling
- Local contact models have also been applied to peridynamic simulations
  - Iterative penalty approach to disallow interpenetration and minimize contact gap
- Contact modeling remains an open research topic in peridynamics

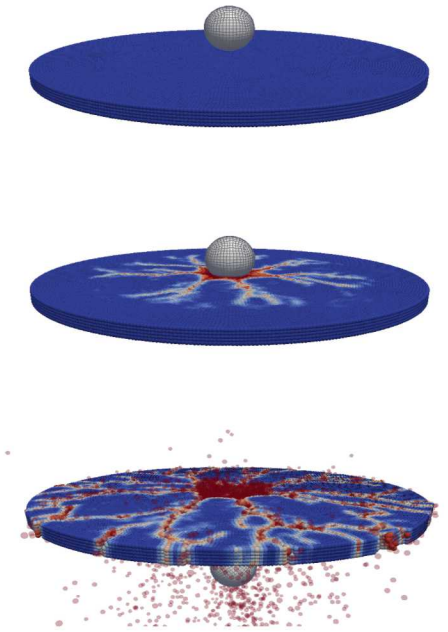

Simulation of brittle fracture

1. Silling, S.A. and Askari, E. A meshfree method based on the peridynamic model of solid mechanics. *Computers and Structures* 83:1526-1535, 2005.
2. SIERRA Solid Mechanics Team, Sierra/SolidMechanics 4.22 user's guide, SAND Report 2011-7597, Sandia National Laboratories, Albuquerque, NM and Livermore, CA, 2011.

Short-range force contact models

- Spring-like repulsive force
- Active when relative distance is smaller than the prescribed contact radius
- Does not require explicit definition of contact surfaces
- Interpenetration is possible (high velocity, node misalignment)
- Friction may be incorporated by decomposing relative motion into normal and tangential components

Example of a short-range force contact model

Force is zero if distance between nodes is greater than d_{ij}

$$d_{ij} = \min\left\{\beta|\mathbf{x}_j - \mathbf{x}_i|, \alpha(r_i + r_j)\right\}$$

Short-range force includes static and dynamic components

$$\mathbf{f}_{\text{static}} = \mathrm{A}\,\mathrm{C}_{ij}\left(\frac{\mathrm{d} - |\mathbf{y}_j - \mathbf{y}_i|}{\mathrm{d}}\right)\,\Delta V_i\,\Delta V_j\,\mathbf{M}_{ij}$$

$$\mathrm{C}_{ij} = \frac{18\mathrm{k}}{\pi\delta^4} \qquad \mathbf{M}_{ij} = \frac{\mathbf{y}_j - \mathbf{y}_i}{|\mathbf{y}_j - \mathbf{y}_i|}$$

$$\mathbf{f}_{\text{damping}} = \epsilon\,\gamma_c\,v_{ij}\,\mathbf{M}_{ij}$$

$$v_{ij} = (\mathbf{v}_j - \mathbf{v}_i)\cdot\mathbf{M}_{ij}$$

$$\gamma_c = 2\sqrt{A\,\mathrm{C}_{ij}\,\Delta V_i\,\Delta V_j\,\bar{m}}$$

Illustration of short range force and standard bond force

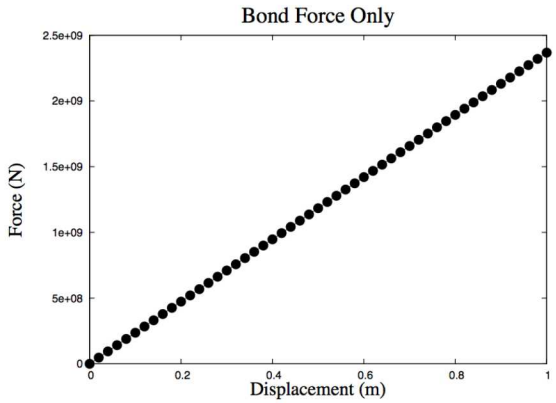

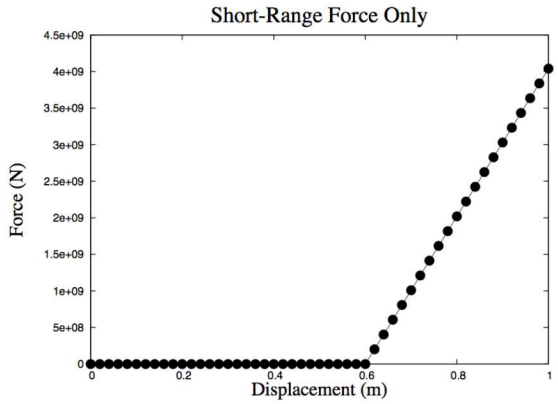

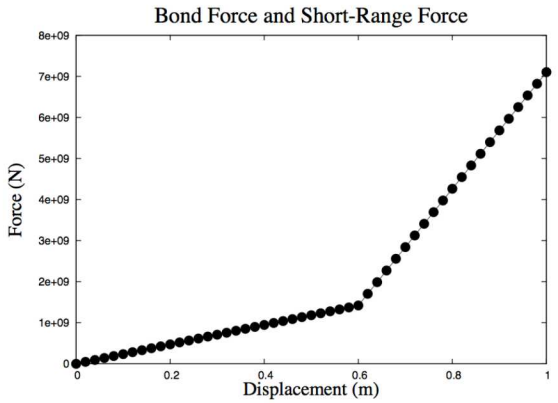

Applying a traditional (local) contact model to peridynamics

- Contact algorithm operates on planar facets
- Peridynamics algorithm operates on sphere elements
- Lofted geometry allows for coupling of peridynamics and contact algorithm

Initial hex mesh | Conversion to sphere mesh | Create planar facets for contact algorithm

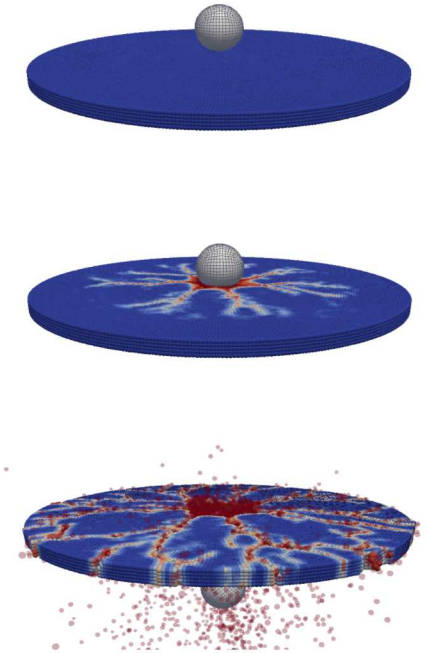

Simulation of brittle fracture

D. J. Littlewood. Simulation of dynamic fracture using peridynamics, finite element modeling, and contact. In *Proceedings of the ASME 2010 International Mechanical Engineering Congress and Exposition (IMECE)*, Vancouver, British Columbia, Canada, 2010.

SIERRA Solid Mechanics Team. Sierra/SolidMechanics 4.36 user's guide. SAND Report 2015-2199, Sandia National Laboratories, Albuquerque, NM and Livermore, CA.

Challenges with contact and nonlocal models

Simple test: To bars in contact and under compression

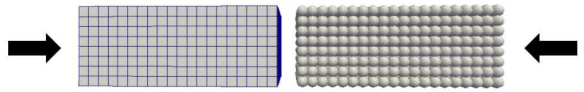

Horizon = 3 * Mesh Spacing

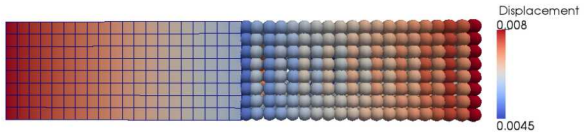

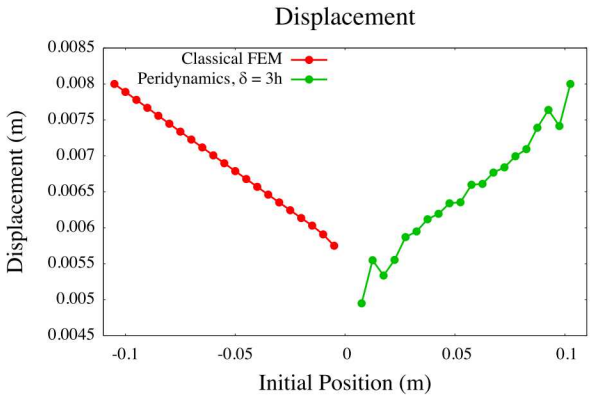

Horizon = Mesh Spacing

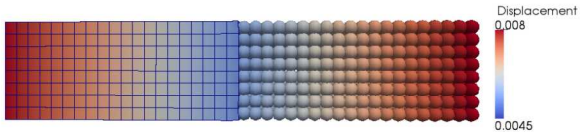

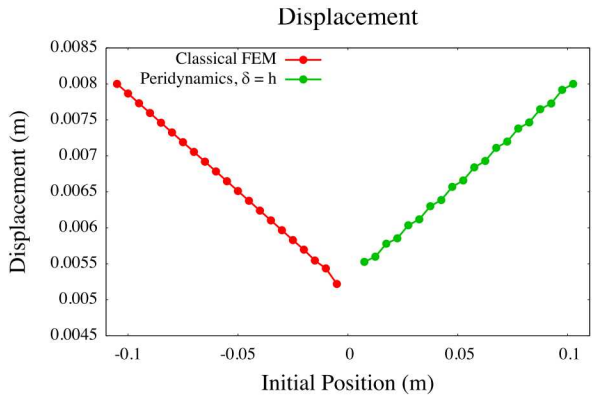

Meshfree discretizations for peridynamics

- Meshfree discretization is defined by nodal volumes: **(x, y, z, V)**
- Each nodal volumes is assigned a material model, etc.
  - Nodal volumes may be grouped into ”blocks” to simplify bookkeeping
- Example approaches for generating a meshfree discretization:
  - Simulation code internal mesh generator
  - Pre-processing script to generate (x,y,z,V) data
  - Conversion of a FEM hex/tet mesh to nodal volumes
- Concerns specific to peridynamics:
  - A variable horizon is generally not supported in peridynamics
  - Discretization can be nonuniform, but large variations in V can produce undesirable results
  - Boundary conditions are generally applied over a volumetric region; bookkeeping can be challenging, thin layers can cause difficulty

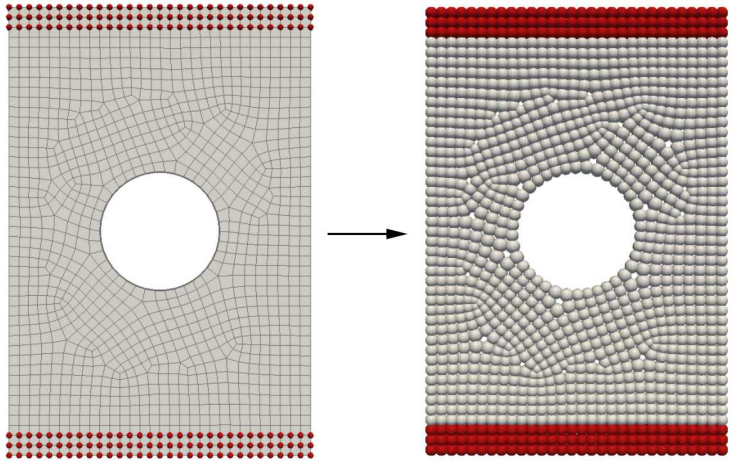

Conversion of a FEM mesh to a meshfree discretization

- Node sets defined in the original hex/tet mesh must be transferred to meshless discretization
  - Elements are preserved (one-to-one map) but nodes in the FEM mesh are not preserved
- A mechanism is required for treating small features, controlling visibility between material points
  - A so-called bond filter may be used to disallow pairwise interactions

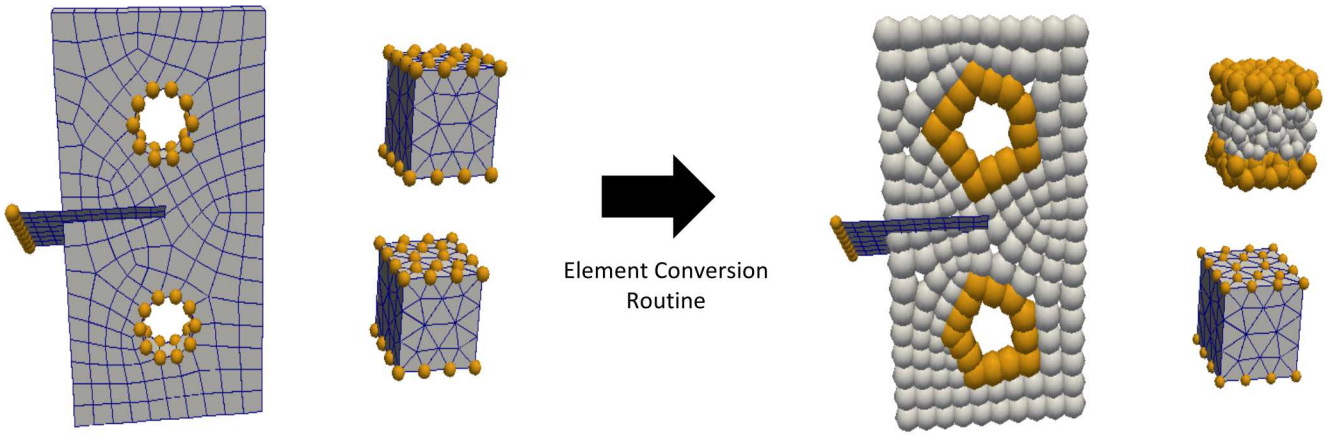

Initial mesh generated in Cubit

Peridynamic blocks converted to sphere elements

Time integration for computational solid mechanics

- Explicit integration (dynamics): Velocity-Verlet, a.k.a. leapfrog
  - Well suited for modeling pervasive damage
  - Does not require the solution of a global system of equations
  - Conditionally stable, requires small time step
  - Equivalent to Newmark Beta with Beta = 0, gamma = 0.5
- Implicit integration for quasi-statics
  - Assumes that acceleration is zero everywhere, solve for equilibrium
  - Wave propagation is neglected
  - Requires solution of a global system of equations
  - Care must be taken w.r.t. rigid body modes
- Implicit integration for dynamics
  - Newmark Beta
  - Requires solution of a global system of equations

Explicit time integration

- Appropriate for dynamic problems and those with pervasive material failure

$$\rho(\mathbf{x})\ddot{\mathbf{u}}_h(\mathbf{x},t) = \sum_{i=0}^{N} \left\{ \underline{\mathbf{T}}[\mathbf{x},t]\left\langle \mathbf{x}'_i - \mathbf{x} \right\rangle - \underline{\mathbf{T}}'[\mathbf{x}'_i,t]\left\langle \mathbf{x} - \mathbf{x}'_i \right\rangle \right\} \Delta V_{\mathbf{x}'_i} + \mathbf{b}(\mathbf{x},t)$$

- Conditionally stable
- Requires estimate of the critical time step
- Requires many small time steps
- Easy to implement
- Does not require solution of global system of equations

Algorithm 1 Velocity Verlet

1: $\mathbf{v}^{n+1/2} = \mathbf{v}^n + \frac{\Delta t}{2}\mathbf{M}^{-1}(\mathbf{f}^n + \mathbf{b}^n)$
2: $\mathbf{u}^{n+1} = \mathbf{u}^n + \Delta t \mathbf{v}^{n+1/2}$
3: $\mathbf{v}^{n+1} = \mathbf{v}^{n+1/2} + \frac{\Delta t}{2}\mathbf{M}^{-1}(\mathbf{f}^{n+1} + \mathbf{b}^{n+1})$

Implicit time integration

- Unconditionally stable
- Allows for large time steps
- Suitable for solution of static and quasi-static problems
- Suitable for implicit dynamics
- Requires solution of system of equations involving current and future configurations
  - Generally nonlinear
  - Newton-like methods require tangent stiffness matrix
  - Matrix-free schemes offer a promising alternative approach (e.g., Jacobian-Free Newton-Krylov)

S. A. Silling. Linearized theory of peridynamic states. *Journal of Elasticity*, 99:85–111, 2010.

J. A. Mitchell. A nonlocal, ordinary, state-based plasticity model for peridynamics. SAND Report 2011-3166, Sandia National Laboratories, Albuquerque, NM and Liver- more, CA, 2011.

M.L. Parks, D.J. Littlewood, J.A. Mitchell, and S.A. Silling, Peridigm Users' Guide v1.0.0. Sandia Report SAND2012-7800, 2012.

Brothers, M.D., Foster, J.T., and Millwater, H.R. A comparison of different methods for calculating tangent-stiffness matrices in a massively parallel computational peridynamics code. *Computer Methods in Applied Mechanics and Engineering* 279:247-267, 2014.

David J. Littlewood. Roadmap for Peridynamic Software Implementation. SAND Report 2015-9013. Sandia National Laboratories, Albuquerque, NM and Livermore, CA, 2015.

The tangent stiffness matrix

- Approaches for construction:
  - Analytic (i.e., peridynamic modulus state)
  - Finite difference
  - Automatic differentiation
- Tangent is expensive
  - Expensive to construct
  - Expensive to store
  - Expensive to apply
- Number of nonzeros is directly related to the number of peridynamic bonds
  - Nonzero entry for all bonded nodes
  - Nonzero entry for all nodes that are bonded to a common node (state based)

Algorithm 1 Construction of the tangent stiffness matrix by central finite difference.

procedure TANGENT STIFFNESS MATRIX
  ▷ Initialize the tangent stiffness matrix to zero.
  $\mathbf{K} \leftarrow \mathbf{0}$
  ▷ Traverse each node in the discretization.
  for each node i **do**
    $\{traversal\ list\} \leftarrow$ node i and all neighbors of node i
    for each node j in $\{traversal\ list\}$ **do**
      ▷ Evaluate the force state at $\mathbf{x}_i$ under perturbations of displacement.
      for each displacement degree of freedom r at node j **do**
        $\underline{\mathbf{T}}^{\epsilon+} \leftarrow \underline{\mathbf{T}}[\mathbf{x}_i](\mathbf{u} + \boldsymbol{\epsilon}^r)$
        $\underline{\mathbf{T}}^{\epsilon-} \leftarrow \underline{\mathbf{T}}[\mathbf{x}_i](\mathbf{u} - \boldsymbol{\epsilon}^r)$
        ▷ Evaluate pairwise forces under perturbations of displacement.
        for each node k in neighbor list of node i **do**
          $\boldsymbol{f}^{\epsilon+} \leftarrow \underline{\mathbf{T}}^{\epsilon+}\langle \mathbf{x}_k - \mathbf{x}_i \rangle\ \Delta V_i\ \Delta V_k$
          $\boldsymbol{f}^{\epsilon-} \leftarrow \underline{\mathbf{T}}^{\epsilon-}\langle \mathbf{x}_k - \mathbf{x}_i \rangle\ \Delta V_i\ \Delta V_k$
          $\boldsymbol{f}^{\text{diff}} \leftarrow \boldsymbol{f}^{\epsilon+} - \boldsymbol{f}^{\epsilon-}$
          for each degree of freedom s at node k **do**
            $\mathrm{K}_{sr} \leftarrow \mathrm{K}_{sr} + \frac{f_s^{\text{diff}}}{2\epsilon}$
          end for
        end for
      end for
    end for
  end for
end procedure

Outline

- Ingredients of a peridynamics simulation
  - Governing equations
  - Constitutive model, bond failure law
  - Contact model
  - Discretization
  - Time integrator
- **Surface effect in peridynamic simulations**
- Estimation of the maximum stable time step for dynamic simulations
- Convergence of peridynamic models
- Demonstration of meshfree peridynamics for model analysis
- Modeling damage and failure

The peridynamic surface effect is a significant concern for engineering applications

- The majority of peridynamic material models were derived based on bulk response
- Material points close to the surface have a reduced nonlocal region (fewer bonds) relative to material points in the bulk
- Ordinary peridynamic material models exhibit inconsistencies at the surface

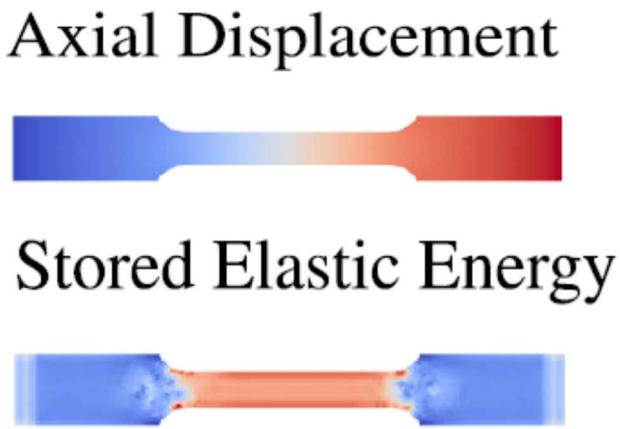

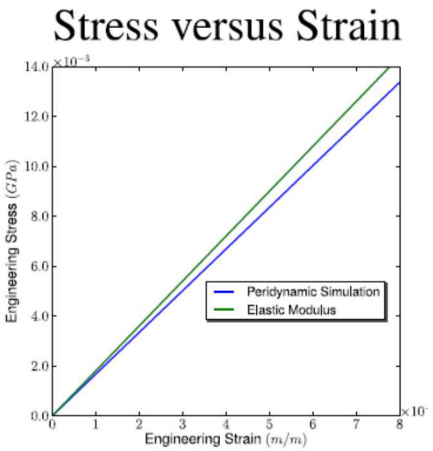

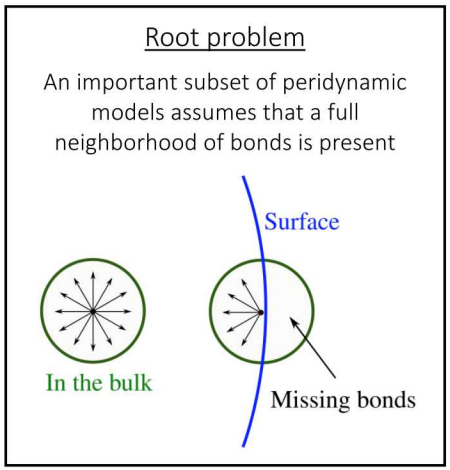

[Images courtesy John Mitchell]

One possible approach to mitigating the surface effect

- **Position-Aware Linear Solid** (PALS) constitutive model takes proximity to free surfaces into account

$$W = \frac{1}{2}K\theta^2 + \mu(\underline{\sigma\varepsilon}) \bullet \underline{\varepsilon}, \qquad \theta = (\underline{\omega}|X|) \bullet \underline{e}$$

- Coefficients σ and ω are determined for each point in the discretized model
- Calculation of σ and ω ensures that the expected strain energy is recovered for a set of *matching deformations*

Example calculation

PALS model accurately recovers elastic modulus in tensile test

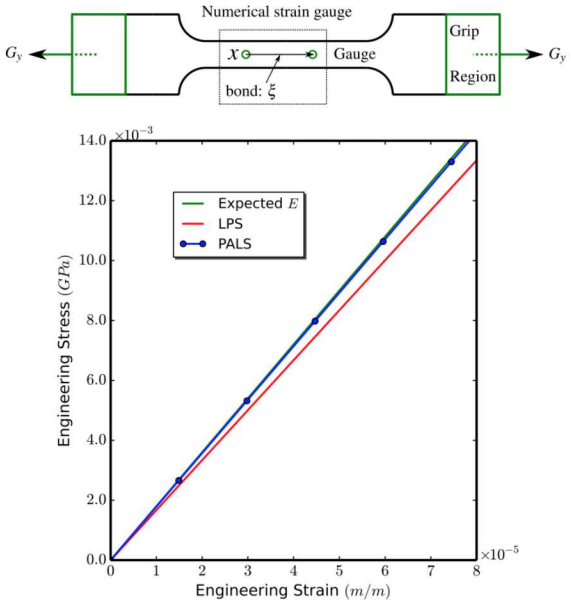

J. Mitchell, S. Silling, and D. Littlewood. A position-aware linear solid (PALS) model for isotropic elastic materials. *Journal of Mechanics of Materials and Structures* 10(5):539-557, 2015.

Outline

- Ingredients of a peridynamics simulation
  - Governing equations
  - Constitutive model, bond failure law
  - Contact model
  - Discretization
  - Time integrator
- Surface effect in peridynamic simulations
- **Estimation of the maximum stable time step for dynamic simulations**
- Convergence of peridynamic models
- Demonstration of meshfree peridynamics for model analysis
- Modeling damage and failure

Candidate approaches for estimating the maximum stable time step

- Courant-Friedrichs-Lewy (CFL) condition

$$c = \sqrt{\frac{k}{\rho}} \qquad \Delta t \leq \frac{\Delta x}{c}$$

- Approach of Silling and Askari for microelastic materials (von Neumann analysis)

$$\Delta t_c = \sqrt{\frac{2\rho}{\sum_p V_p C_{ip}}} \qquad C_{ip} = |\mathbf{C}(x_p - x_i)| = \left|\frac{\partial \mathbf{f}}{\partial \boldsymbol{\eta}}\right|$$

- Global estimate using eigenvalue analysis (via Lanczos method)

$$\mathbf{M}\ddot{\mathbf{u}} + \mathbf{K}\mathbf{u} = \mathbf{f} \qquad (\mathbf{K} - \lambda \mathbf{M})\,\mathbf{x} = 0 \qquad \Delta t_c = \frac{2}{\sqrt{\lambda}}$$

Littlewood, D.J., Thomas, J.D., and Shelton, T.R. Estimation of the critical time step for peridynamic models. Presented at the SIAM Conference on Mathematical Aspects of Materials Science, Philadelphia, Pennsylvania, 2013.

Computational Peridynamics

3. Estimation of the maximum stable time step

- Critical time step for simulation of wave propagation
  - Compared approaches for estimating the maximum stable time step against empirical observations
  - CFL limit with element size as the length scale, and the method of Silling & Askari were conservative
  - Lanczos method was very accurate (but expensive)
  - CFL limit with the horizon as the length scale was unstable

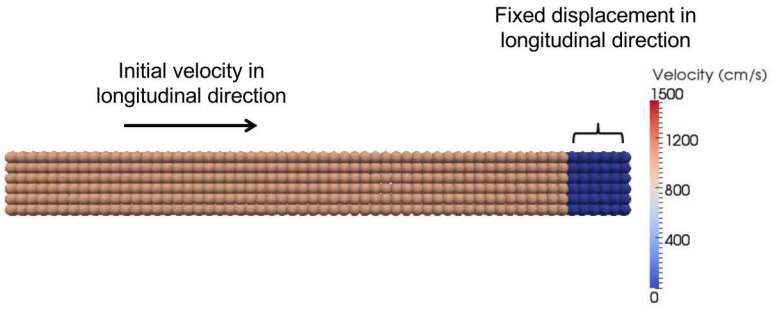

Time Step	Kinetic Energy
0.1 μs	3.51 J
0.2 μs	3.51 J
0.3 μs	3.51 J
0.4 μs	3.51 J
0.5 μs	14.1 J
0.6 μs	NaN
0.7 μs	NaN
0.8 μs	NaN
0.9 μs	NaN
1.0 μs	1.75e+299 J

Silling and Askari
max. time step = 0.241 µs
max. kinetic energy = 3.51 J

CFL Limit (element size)
max. time step = 0.329 µs
max. kinetic energy = 3.51 J

Empirical Observation
max. time step = 0.499 µs
max. kinetic energy = 3.51 J

Global Lanczos
max. time step = 0.500 µs
max. kinetic energy = 3.51 J

CFL Limit (horizon)
max. time step = 1.00 µs
max. kinetic energy = unstable

Computational Peridynamics

3. Estimation of the maximum stable time step

Time Step	Percentage of Broken Bonds	Maximum Kinetic Energy ($t > 10\ \mu s$)
0.01 μs	44.3 %	3.83 kJ
0.1 μs	44.5 %	3.82 kJ
0.2 μs	44.7 %	3.82 kJ
0.3 μs	45.3 %	3.82 kJ
0.4 μs	45.3 %	3.82 kJ
0.5 μs	45.4 %	3.82 kJ
0.6 μs	46.7 %	3.81 kJ
0.7 μs	49.1 %	3.83 kJ
0.8 μs	73.5 %	3.82 kJ
0.9 μs	95.3 %	4.39 kJ
1.0 μs	99.1 %	6.40 kJ

Silling and Askari

max. time step = 0.290 μs
percentage of broken bonds = 44.7 %
max. kinetic energy = 3.82 kJ

CFL Limit (element size)

max. time step = 0.395 μs
percentage of broken bonds = 45.3 %
max. kinetic energy = 3.51 J

Global Lanczos

max. time step = 0.682 μs
percentage of broken bonds = 46.0 %
max. kinetic energy = 3.83 kJ

Empirical Observation

max. time step = 0.707 μs
percentage of broken bonds = 50.0 %
max. kinetic energy = 3.83 kJ

CFL Limit (horizon)

max. time step = 1.19 μs
percentage of broken bonds = 99.1 %
max. kinetic energy = unstable

Time step = 5.0 μs
46.7% of bonds broken

Time step = 7.5 μs
62.7 % of bonds broken

Computational Peridynamics

3. Estimation of the maximum stable time step

- Choice of influence function affects critical time step
- Lanczos algorithm successfully detects changes in critical time step
- Observation: Influence function that decays with increasing bond length results in reduced critical time step

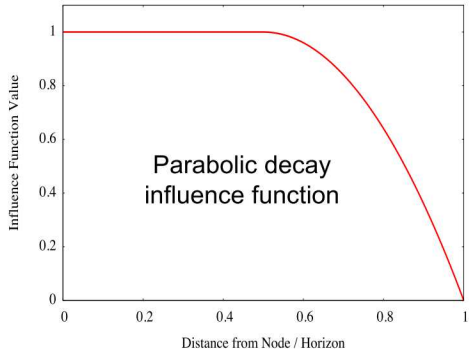

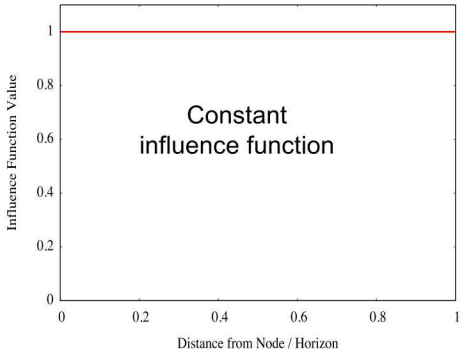

Peridynamic Linear Solid

	Parabolic decay influence function	Constant influence function
Max. Lanczos time step	0.381 μs	0.434 μs
Empirical result	0.381 μs	0.434 μs

14% Increase

Correspondence Material Model

	Parabolic decay influence function	Constant influence function
Max. Lanczos time step	0.490 μs	0.549 μs
Empirical result	0.490 μs	0.549 μs

12% Increase

Outline

- Ingredients of a peridynamics simulation
  - Governing equations
  - Constitutive model, bond failure law
  - Contact model
  - Discretization
  - Time integrator
- Surface effect in peridynamic simulations
- Estimation of the maximum stable time step for dynamic simulations
- **Convergence of peridynamic models**
- Demonstration of meshfree peridynamics for model analysis
- Modeling damage and failure

Convergence of meshfree peridynamics

- Two forms of convergence: horizon and mesh spacing
  - Convergence to a local solution as horizon approaches zero
  - Convergence to a nonlocal solution under mesh refinement with horizon held constant
- Current practice introduces errors and spoils convergence
  - Quadrature, poor treatment of neighbor-horizon intersections

Approaches for improving convergence behavior

- Improved treatment of neighbor-horizon intersections
  - Variety of correction techniques (scalar multiplier):
    - PD-LAMMPS, Hu-Ha-Bobaru, analytic partial area (2D)
  - Application of smoothly-decaying influence functions
  - Approximate calculation of partial volumes (3D)
  - Geometry, quadrature

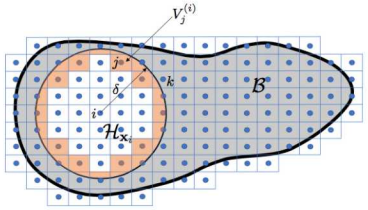

Neighbor-horizon intersection in 2D

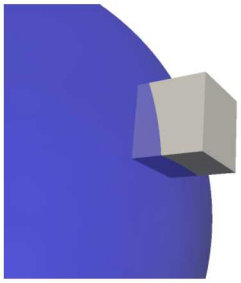

Neighbor-horizon intersection in 3D

Seleson, P. Improved one-point quadrature algorithms for two-dimensional peridynamic models based on analytical calculations, *CMAME*, 282, pp. 184-217, 2014.

Seleson, P., and Littlewood, D.J. Convergence studies in meshfree peridynamic simulations. *Computers and Mathematics with Applications* 71:2432-2448, 2016.

Seleson, P., and David J. Littlewood, D.J. Numerical tools for effective meshfree discretizations of peridynamic models. In George Z. Voyiadjis, editor, *Handbook of Nonlocal Continuum Mechanics for Materials and Structures. Springer. Accepted.*

Explicit calculation of partial areas (2D) and volumes (3D)

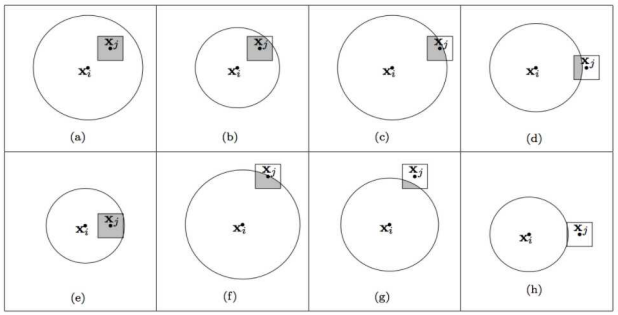

Analytic calculation of partial areas (2D)

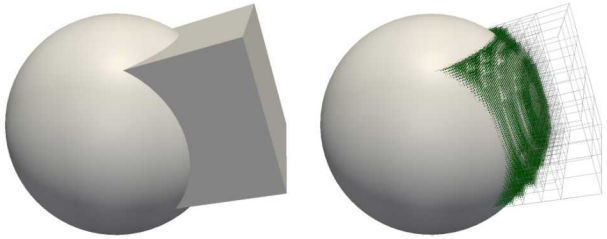

Numerical approximation of partial volumes (3D)

Application of smoothly-decaying influence functions

- Mitigates numerical difficulties at neighbor-horizon interface
- Changes the underlying model (physics)

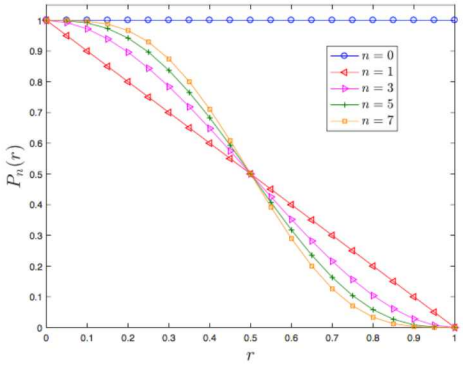

Candidate influence functions

Numerical experiments: Solution of statics problem with known solution

- Linearized LPS material model equates to classical local model under assumption of a quadratic displacement field

Peridynamic equation of static elasticity, linearized LPS model

$$-\int_{\mathcal{H}_{\mathbf{x}}} \frac{\omega(|\boldsymbol{\xi}|)}{m}\Big\{(3K-5G)\left(\vartheta^{\mathrm{lin}}[\mathbf{x}]+\vartheta^{\mathrm{lin}}[\mathbf{x}+\boldsymbol{\xi}]\right)\boldsymbol{\xi} + 30G\frac{\boldsymbol{\xi}\otimes\boldsymbol{\xi}}{|\boldsymbol{\xi}|^2}(\mathbf{u}(\mathbf{x}+\boldsymbol{\xi})-\mathbf{u}(\mathbf{x}))\Big\}\mathrm{d}V_{\boldsymbol{\xi}} = \mathbf{b}(\mathbf{x}) \qquad \mathbf{x}\in\Omega,$$
$$\mathbf{u}(\mathbf{x}) = \mathbf{g}(\mathbf{x}) \qquad \mathbf{x}\in\mathcal{B}\setminus\Omega.$$

Classical Navier-Cauchy equation of static elasticity

$$-\left[G\nabla^2\mathbf{u}(\mathbf{x})+\left(K+\frac{1}{3}G\right)\nabla(\nabla\cdot\mathbf{u})(\mathbf{x})\right]=\mathbf{b}(\mathbf{x}).$$

- Permits verification via method of manufactured solutions

Quadratic displacement field

$$u(\mathbf{x}) = U_{11}x^2+U_{22}y^2+U_{33}z^2+U_{12}xy+U_{13}xz+U_{23}yz,$$
$$v(\mathbf{x}) = V_{11}x^2+V_{22}y^2+V_{33}z^2+V_{12}xy+V_{13}xz+V_{23}yz,$$
$$w(\mathbf{x}) = W_{11}x^2+W_{22}y^2+W_{33}z^2+W_{12}xy+W_{13}xz+W_{23}yz,$$

Body force density for static equilibrium

$$b_1 = -\left[2G\left(U_{11}+U_{22}+U_{33}\right)+\left(K+\frac{1}{3}G\right)\left(2U_{11}+V_{12}+W_{13}\right)\right],$$
$$b_2 = -\left[2G\left(V_{11}+V_{22}+V_{33}\right)+\left(K+\frac{1}{3}G\right)\left(U_{12}+2V_{22}+W_{23}\right)\right],$$
$$b_3 = -\left[2G\left(W_{11}+W_{22}+W_{33}\right)+\left(K+\frac{1}{3}G\right)\left(U_{13}+V_{23}+2W_{33}\right)\right].$$

Numerical experiments: Solution of statics problem with known solution

- Cubic computational domain
- U_{11} nonzero, all other components of quadratic displacement field set to zero
- Displacement prescribed over boundary layer
- Body force applied to inner region
- Solution for inner region should converge to the analytic solution under mesh refinement (horizon fixed)

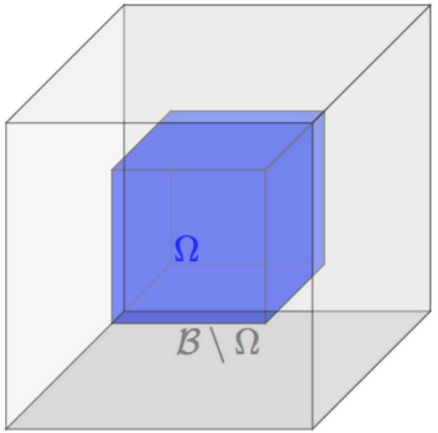

Convergence results for different partial-volume schemes and different influence functions

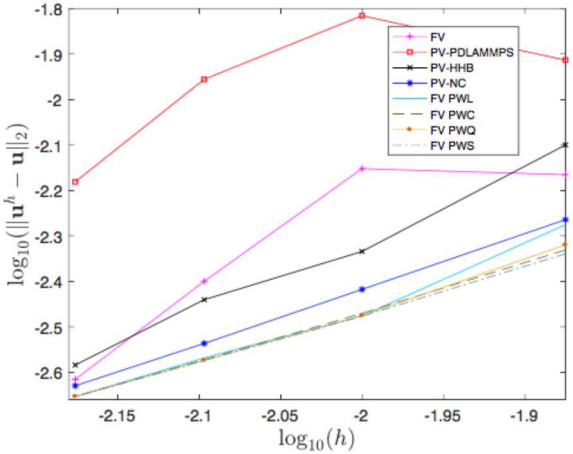

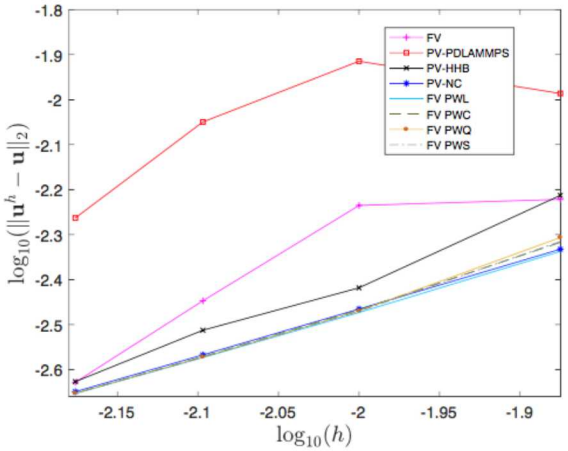

Algorithm	$\alpha = 0$		$\alpha = 1$	
	$\bar{r}$	R	$\bar{r}$	R
FV	1.53	0.165	1.38	0.128
PV-PDLAMMPS	0.86	0.186	0.89	0.167
PV-HHB	1.56	0.035	1.34	0.030
PV-NC	1.22	0.003	1.05	0.001
FV PWL	1.24	0.036	1.05	0.004
FV PWC	1.07	0.005	1.11	0.009
FV PWQ	1.10	0.014	1.15	0.016
FV PWS	1.04	0.006	1.12	0.012

Numerical experiments: Solution of dynamics problem

- Cubic computational domain
- Initial displacement applied to shell of internal nodes
- Wave allowed to propagate freely through domain
- Solutions compared against highly-refined benchmark solution

Initial displacement

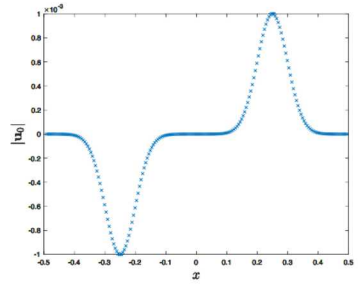

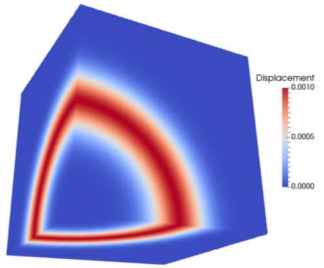

Final displacement

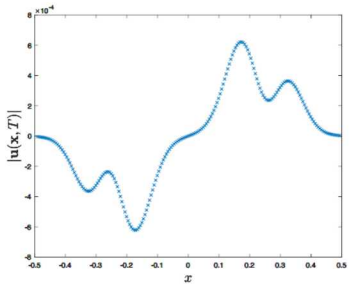

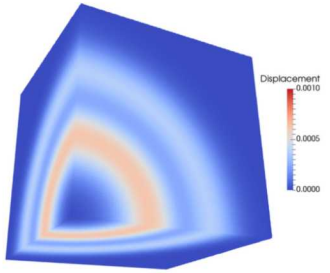

Initial conditions

$$\mathbf{u}_0(\mathbf{x}) = \begin{cases} ae^{-\frac{(|\mathbf{x}|-r_0)^2}{\ell^2}} \frac{\mathbf{x}}{|\mathbf{x}|} & \text{if} \quad (r_0 - 3\ell) \leqslant |\mathbf{x}| \leqslant (r_0 + 3\ell) \\ 0 & \text{otherwise,} \end{cases},$$

$$\mathbf{v}_0(\mathbf{x}) = \mathbf{0},$$

Convergence results for different partial-volume schemes and different influence functions

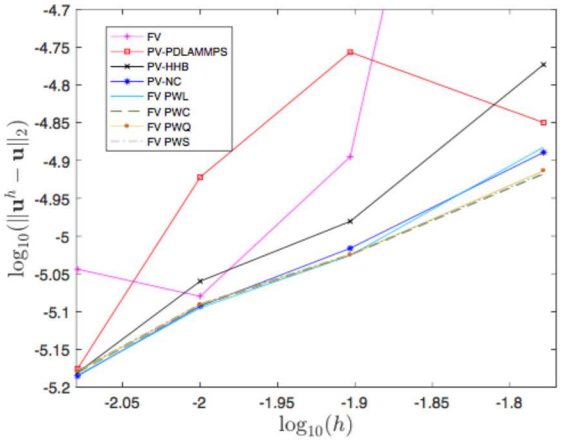

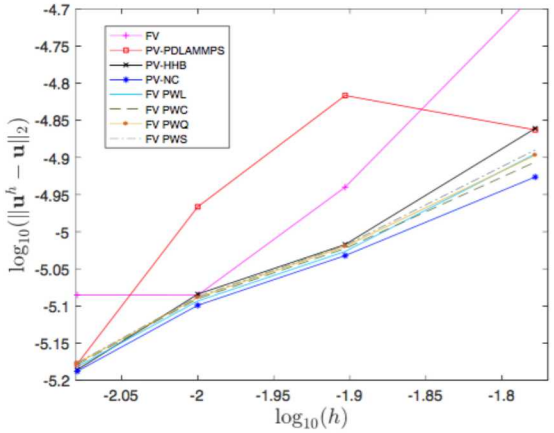

Algorithm	$\alpha = 0$		$\alpha = 1$	
	$\bar{r}$	R	$\bar{r}$	R
FV	4.27	0.514	1.41	0.099
PV-PDLAMMPS	1.05	0.202	1.02	0.157
PV-HHB	1.31	0.038	1.04	0.026
PV-NC	0.96	0.013	0.85	0.016
FV PWL	0.98	0.019	0.93	0.017
FV PWC	0.85	0.016	0.88	0.015
FV PWQ	0.86	0.015	0.91	0.015
FV PWS	0.85	0.016	0.93	0.015

Changing the influence function changes the underlying model (physics)

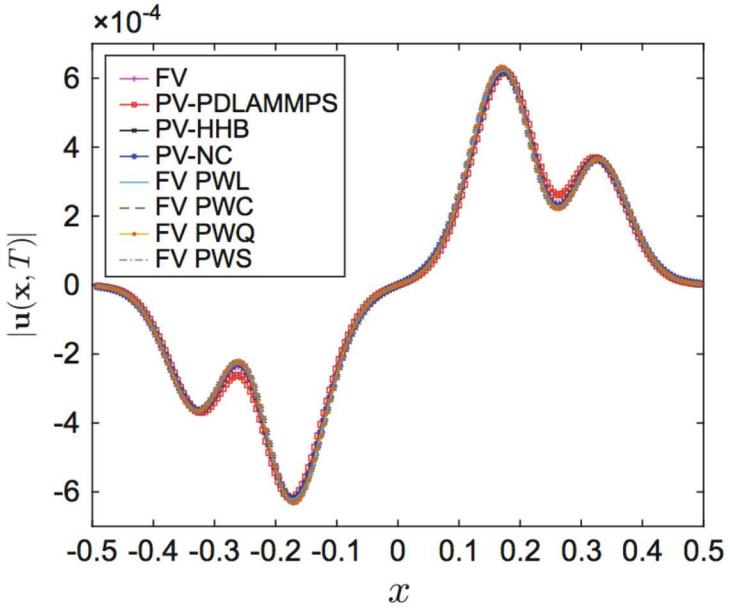

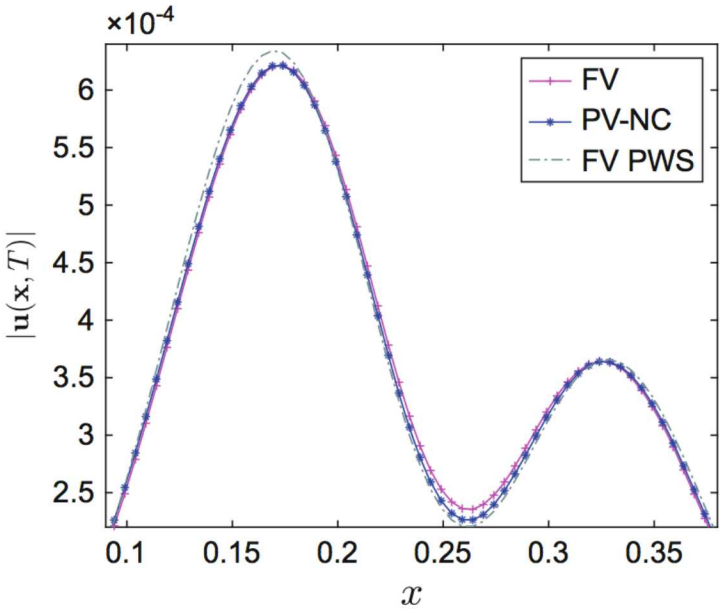

Convergence studies with peridynamic are inherently difficult / expensive

- Volumetric region for prescribed displacement becomes large as horizon increases
- Number of nodes / bonds becomes large as horizon decreases

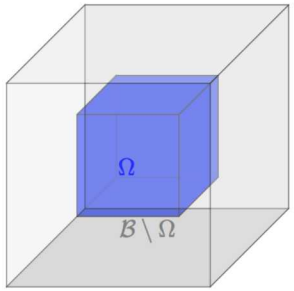

δ/L	0.000	0.001	0.005	0.010	0.050	0.100
$\lvert\mathcal{B} \setminus \Omega\rvert/\lvert\Omega\rvert$	0.000	0.012	0.062	0.130	0.953	3.630

- Number of bonds becomes huge as the ratio of the horizon to the node spacing becomes large

N_{neig} (δ/h)	Number of PD bonds	
	FV	PV-NC
3	12,433,244	25,077,672
4	62,022,592	110,046,364
5	242,986,412	384,681,876
6	753,964,092	1,040,684,328
7	1,838,660,296	2,552,461,732
8	4,080,378,204	5,479,353,788
9	8,456,684,628	10,782,968,496
10	15,752,838,172	19,683,573,672

Outline

- Ingredients of a peridynamics simulation
  - Governing equations
  - Constitutive model, bond failure law
  - Contact model
  - Discretization
  - Time integrator
- Surface effect in peridynamic simulations
- Estimation of the maximum stable time step for dynamic simulations
- Convergence of peridynamic models
- **Demonstration of meshfree peridynamics for model analysis**
- Modeling damage and failure

Why modal analysis?

- Modal analysis is used to determine the dominant structural modes and natural frequencies of a given system
- Peridynamic models containing material damage can be used in the analysis of experimentally-measured frequency responses (nondestructive testing of bridges, etc.)

How does it work?

- Modal analysis is achieved by solving for the dominant eigenvalues and eigenvectors of the tangent stiffness matrix

Test case

One-dimensional analysis of simply-supported beam with square cross section

Classical (local) analytic solution

E	Elastic modulus
h	Height and depth of beam
m	Mass of beam
l	Length of beam
n	Positive integer
f_n	Characteristic linear frequency (mode n)

$$f_n = \frac{n^2\pi}{2}\sqrt{\frac{E\,h^4}{12\,m\,l^4}}$$

Results from peridynamic simulation

- Beam dimensions: 1m x 0.01m x 0.01m
- Material: steel (E = 206.8 GPa)
- Peridynamic horizon: 0.000713m
- Correspondence elastic material model
- Beam discretized with 840K elements

Mode	Classical Theory	Peridynamic Simulation	Percent Difference
1	23.30 Hz	23.26 Hz	0.17 %
2	93.22 Hz	93.02 Hz	0.21 %
3	209.73 Hz	209.06 Hz	0.32 %
4	372.86 Hz	371.29 Hz	0.43 %
5	582.59 Hz	579.39 Hz	0.55 %

Visualization of first five mode shapes

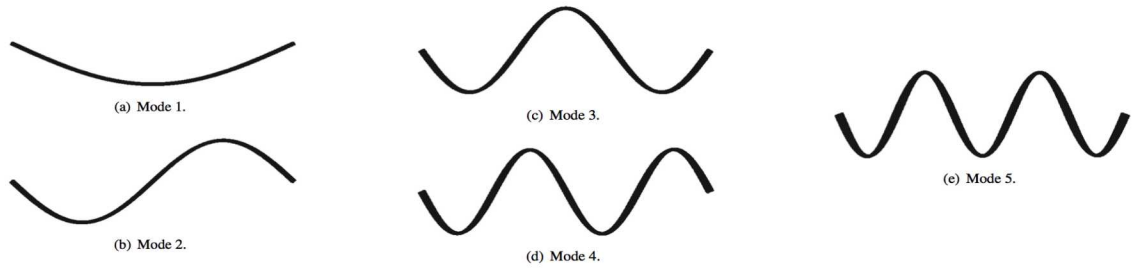

David J. Littlewood, Kyran Mish, and Kendall Pierson. 2012. Peridynamic simulation of damage evolution for structural health monitoring. Proceedings of the ASME 2012 International Mechanical Engineering Congress and Exposition (IMECE2012), Houston, TX.

Outline

- Ingredients of a peridynamics simulation
  - Governing equations
  - Constitutive model, bond failure law
  - Contact model
  - Discretization
  - Time integrator
- Surface effect in peridynamic simulations
- Estimation of the maximum stable time step for dynamic simulations
- Convergence of peridynamic models
- Demonstration of meshfree peridynamics for model analysis
- **Modeling damage and failure**

Modeling failure and damage with peridynamics

- Modeling pervasive damage is a primary advantage of peridynamics
- Nonlocality separates the length scale (horizon) from the mesh, which **relieves mesh dependence**
- **Convergent solutions** to material failure problems (localizing phenomenon) are possible with peridynamics, impossible with a local model
- Cracks develop / grow / branch in peridynamic simulations based primarily on energetics

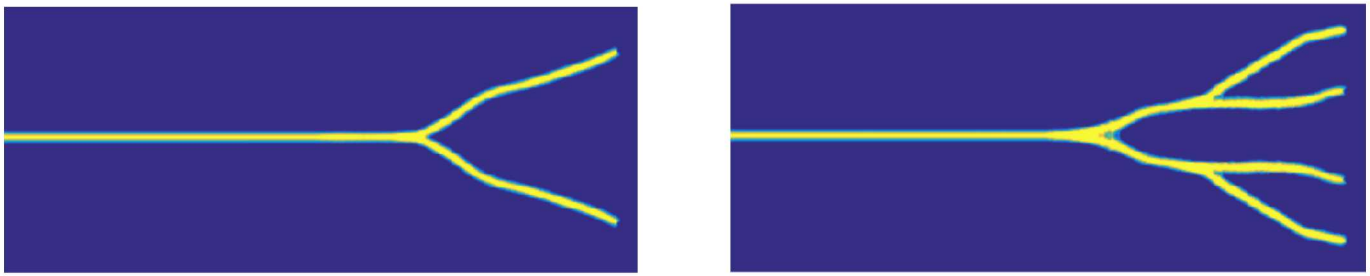

[Images courtesy Seleson]

Experimental setup

- Tube expansion via collision of Lexan projectile and plug within AerMet tube
- Accurate recording of velocity and displacement on tube surface

Modeling approach

- AerMet tube modeled with peridynamics, elastic-plastic material model with linear hardening
- Lexan plugs modeled with traditional FEM, EOS-enabled Johnson-Cook material model

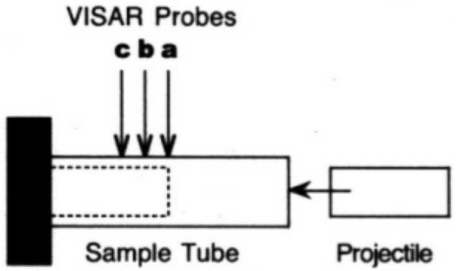

Experimental setup
[Vogler, et al.]

Computational model

Vogler, T.J., Thornhill, T.F., Reinhart, W.D., Chhabidas, L.C., Grady, D.E., Wilson, L.T., Hurricane, O.A., and Sunwoo, A. Fragmentation of materials in expanding tube experiments. *International Journal of Impact Engineering*, 29:735-746, 2003.

D. J. Littlewood. Simulation of dynamic fracture using peridynamics, finite element modeling, and contact. In *Proceedings of the ASME 2010 International Mechanical Engineering Congress and Exposition (IMECE)*, Vancouver, British Columbia, Canada, 2010.

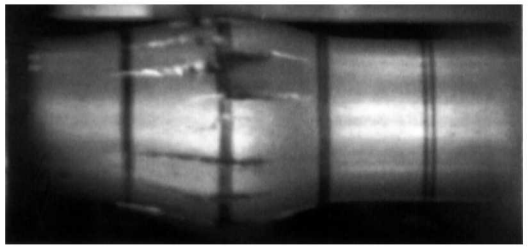

Experimental image at 15.4 microseconds [Vogler et. al]

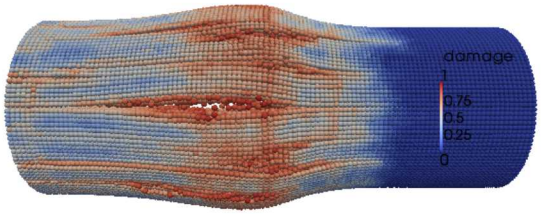

Simulation at 15.4 microseconds

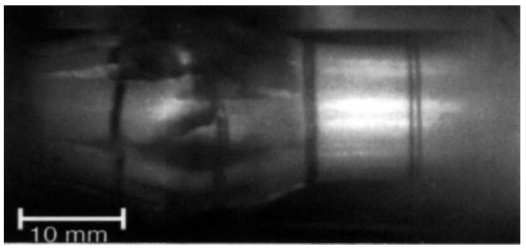

Experimental image at 23.4 microseconds [Vogler et. al]

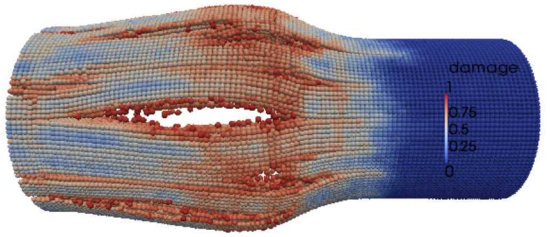

Simulation at 23.4 microseconds

Displacement and velocity
on tube surface
at probe position A

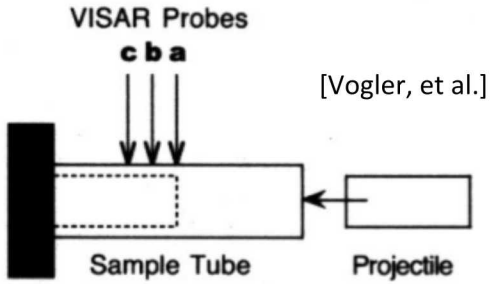

[Vogler, et al.]

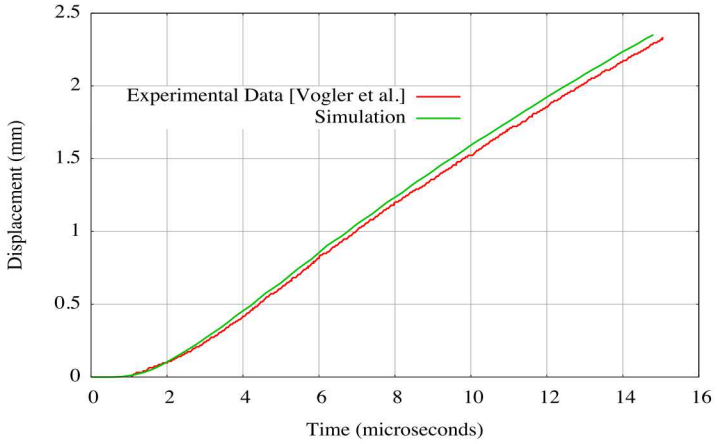

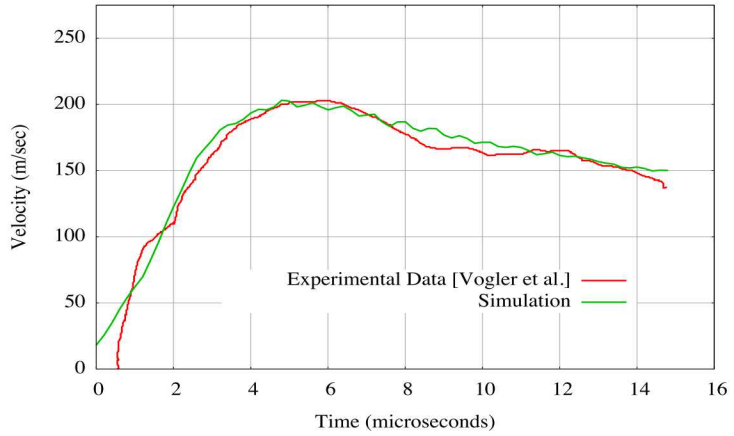

Qualitative Comparison of Fragmentation Results

- Vogler et. al reported significant uncertainty in results at late time
- Approximately half the tube remained intact
- Vogler et al. recovered 14 fragments with mass greater than one gram

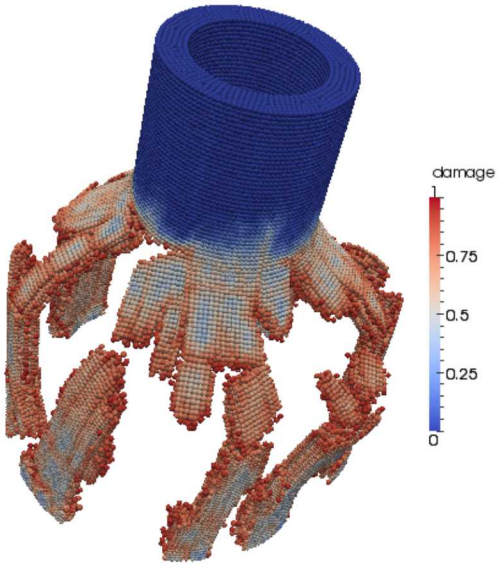

Simulation at 84.8 microseconds

Characterizing fragment data with a Cumulative Distribution Function

- A CDF can be created for any quantity of interest
- Provides insight into the fragmentation process
- Allows for comparison with experimental data

$$P(X) = \frac{1}{M} \sum_{\substack{i=1 \\ X_i \leq X}}^{N_{\text{frag}}} m_i \qquad M = \sum_{i=1}^{N_{\text{frag}}} m_i$$

P(X) is the probability that a given material point belongs to a fragment whose property value X_i is less than *X*

Example: CDF for fragment mass

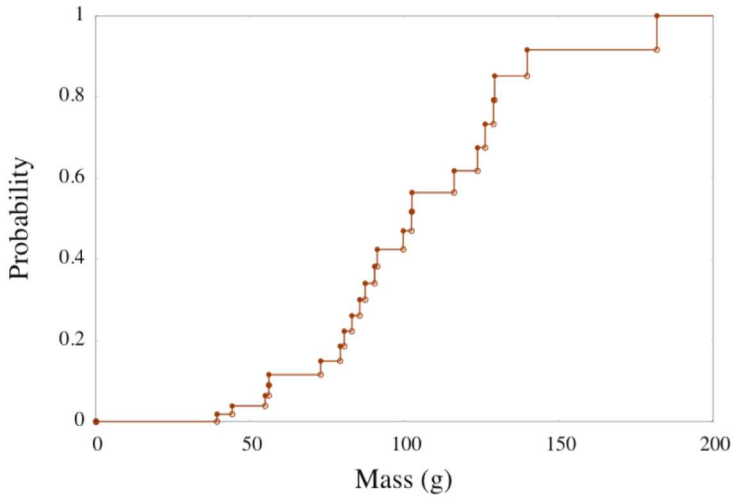

Fragments identification in a meshfree peridynamic simulation

- Provide post-processing capability for characterizing fragmentation process

Approach

- Computational domain is traversed to identify networks of unbroken bonds
- Process is iterative, converges when fragment numbers are no longer changing
- A fragment number is assigned to every node in the model
- Tiny fragments are (optionally) combined and assigned a common fragment number
- Related quantities of interest are computed for each fragment
  - Mass, center of mass, linear and angular momentum, moments of inertia, block names

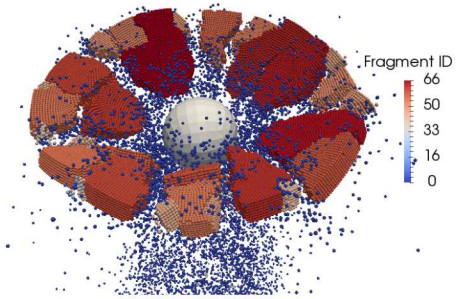

Identification of disk fragments

DO initialize fragment numbers to node ids
REPEAT until fragment numbers stop changing
  FOR every node *i*
    FOR all neighbors *j* of node *i*
      IF the bond between nodes *i* and *j* is unbroken
        DO assign max(F_i , F_j) to nodes *i* and *j*

David Littlewood, Stewart Silling, Paul Demmie. 2016. Identification of Fragments in a Meshfree Peridynamic Simulation. Proceedings of the ASME 2016 International Mechanical Engineering Congress and Exposition, Phoenix, Arizona.

Computational Peridynamics

7. Modeling failure and damage

- Elastic sphere impacting a brittle elastic disk
- Projectile modeled with classical FEM
  - Elastic material model
  - Radius 5.0 mm,
  - Initial velocity 35.0 m/s
- Target modeled with peridynamics
  - Bond-based microelastic material model
  - Critical stretch bond failure rule
  - Radius 17.0 mm, height 2.5 mm

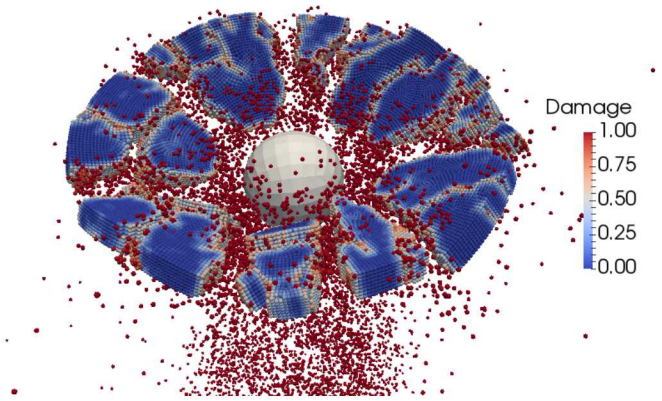

Material parameters for projectile

Parameter	Value
Density ρ	993.1 kg/m^3
Bulk modulus k	1.0 GPa
Poisson's ratio ν	0.3

Material parameters for target

Parameter	Value
Density ρ	2200.0 kg/m^3
Bulk modulus k	14.9 GPa
Horizon δ	1.0 mm
Critical stretch s_{crit}	0.0005

Parameters for fragment identification

output file = frag_data.csv

increment = 4.0e-5

minimum fragment size = 5

Algorithm captures evolution of fragmentation process

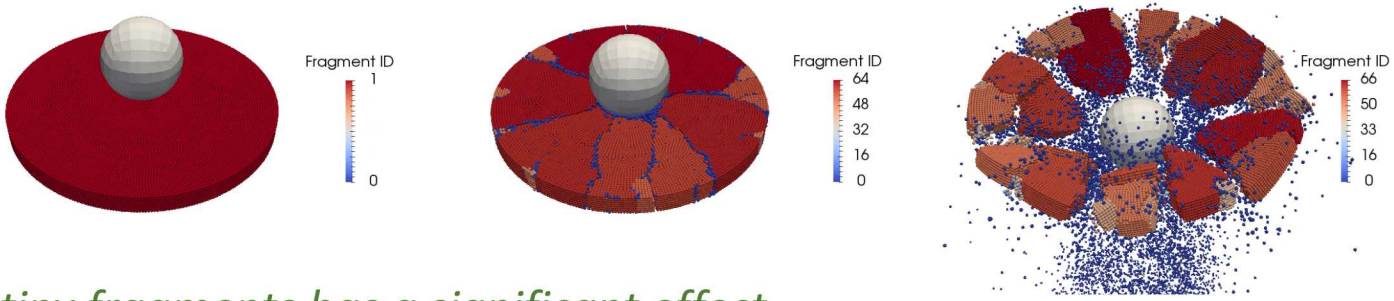

Exclusion of tiny fragments has a significant effect

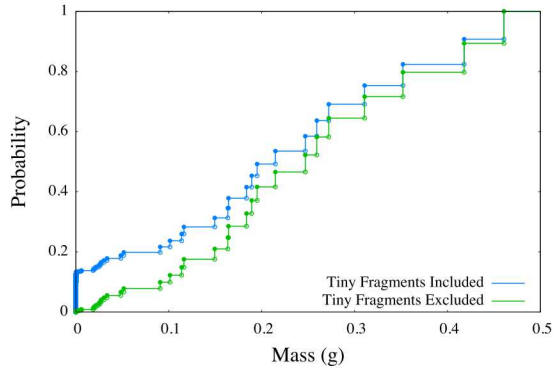

Threshold Fragment Size	Total Mass of Tiny Fragments
1	0.000 g
2	0.531 g
3	0.613 g
4	0.641 g
5	0.651 g

- Fragmentation of an expanding ductile ring
- Bond-based microplastic material model
- Critical stretch bond failure rule
- Inner radius 110.0 mm, outer radius 125.0 mm, height 25.0 mm
- Initial outward radial velocity 100.0 m/s
- ~60,000 nodal volumes

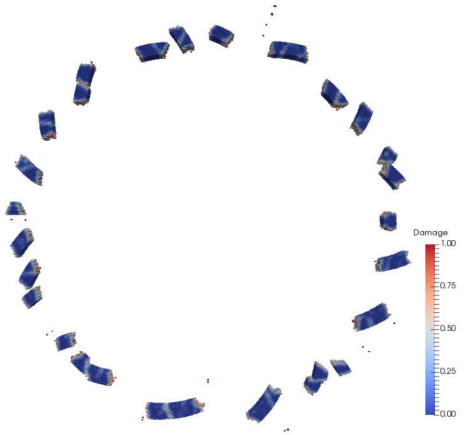

Discretization of ring

Material parameters

Parameter	Value
Density ρ	7850.0 kg/m^3
Bulk modulus k	140.0 GPa
Horizon δ	5.025 mm
Yield stretch s_Y	0.000988
Critical stretch s_{crit}	0.02

Parameters for fragment identification

output file = frag_data.csv
increment = 2.4e-5
minimum fragment size = 0

Algorithm captures evolution of fragmentation process

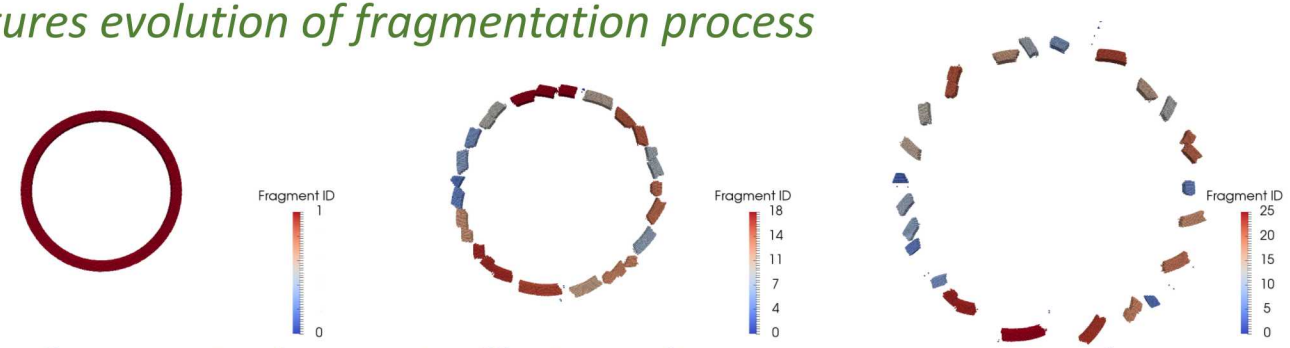

Exclusion of tiny fragments does not affect results

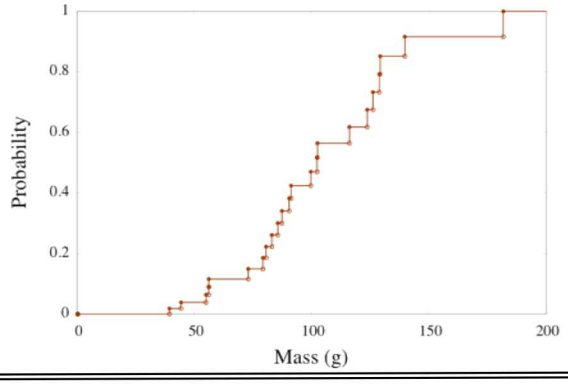

Visualization of fragment momentum

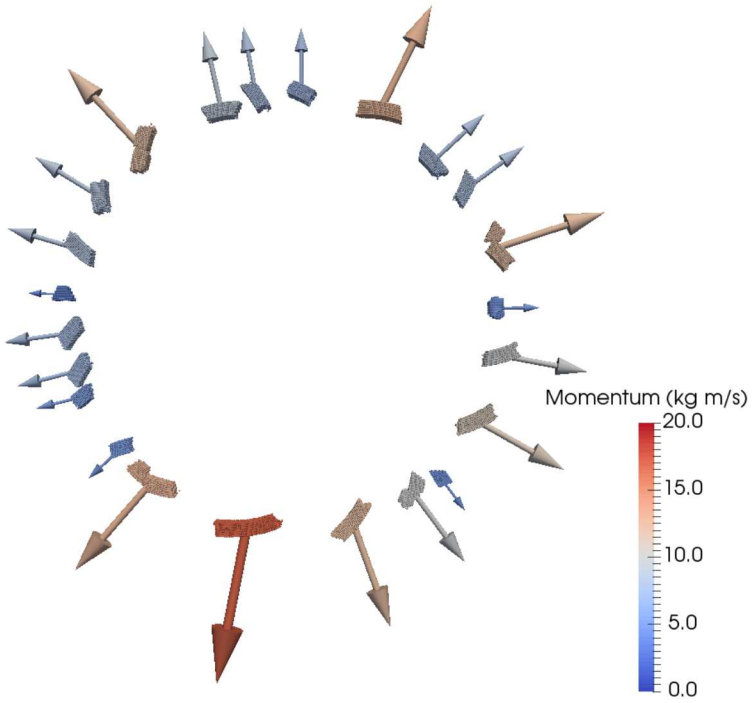

The Peridigm Peridynamics Code

The Peridigm Peridynamics Code

Outline

- Introduction
- Example simulations
  - Tensile test
  - Disk impact
- Hands-on examples

What is Peridigm?

- Open-source software developed at Sandia National Laboratories
- C++ code based on Sandia's *Trilinos* project
- Platform for multi-physics peridynamic simulations
- Capabilities:
  - State-based constitutive models
  - Implicit and explicit time integration
  - Contact for transient dynamics
  - Large-scale parallel simulations
- Compatible with pre- and post-processing tools
  - Cubit mesh generation
  - Paraview visualization tools
  - SEACAS utilities
- Designed for extensibility

https://peridigm.sandia.gov

https://trilinos.org

Design goals

- State-based peridynamics
- Explicit and Implicit time integration
- Contact
- Massively parallel
- Performance
- Extensibility

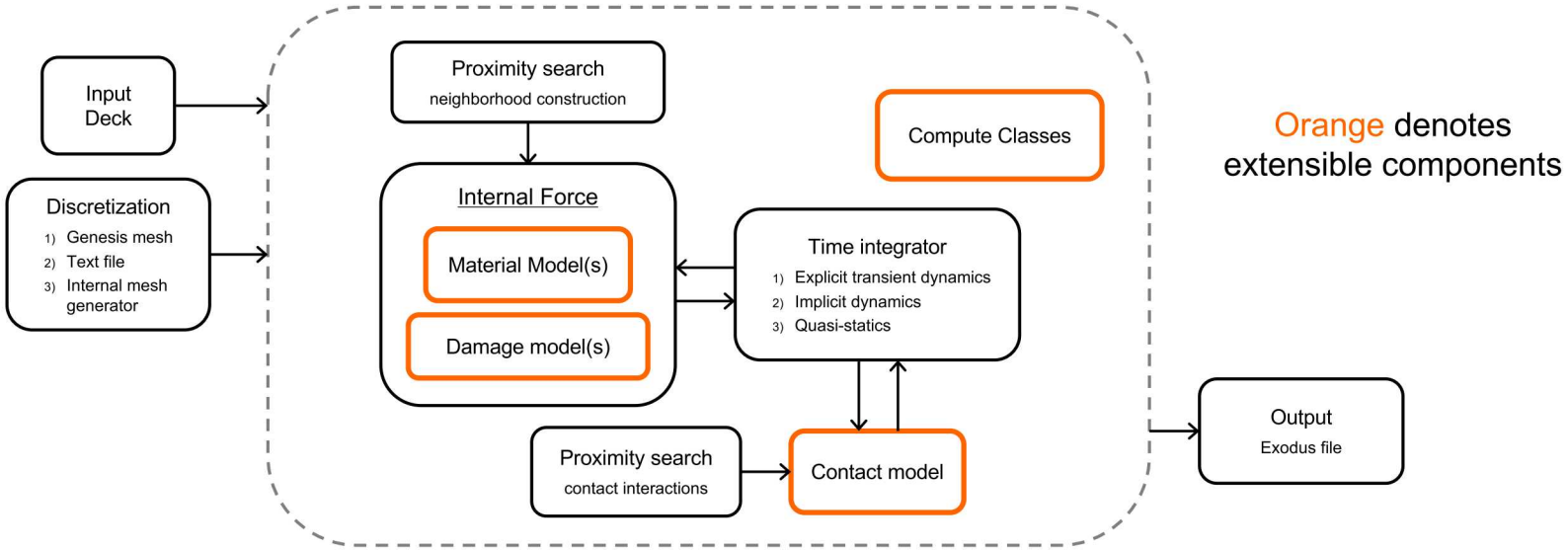

Obtaining the Peridigm source code

http://peridigm.sandia.gov

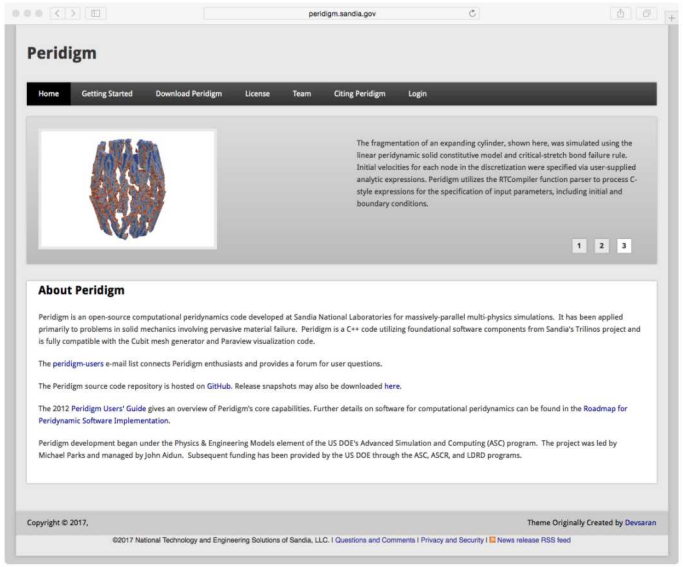

https://github.com/peridigm/peridigm

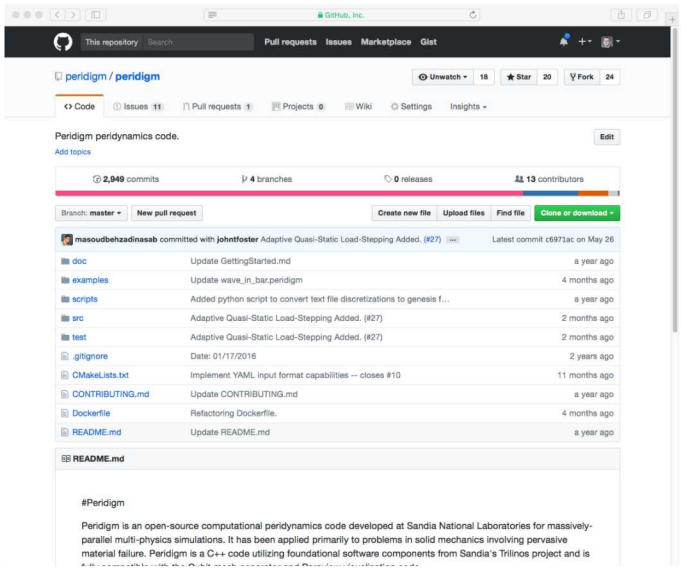

Peridigm Tutorial

1. Introduction

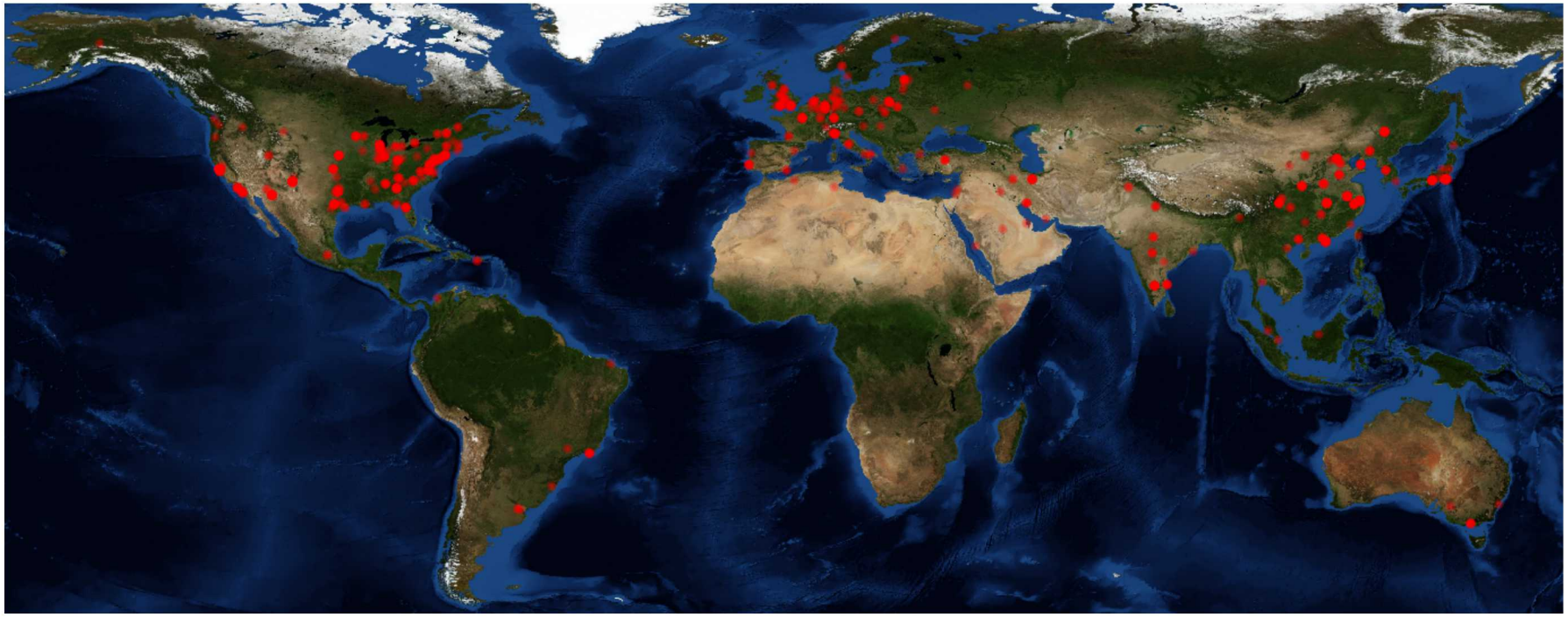

Peridigm Downloads from http://peridigm.sandia.gov (July 2014 – June 2017)

Peridigm Input

- Input deck (text file)
- Discretization (mesh, can be text file or genesis file)

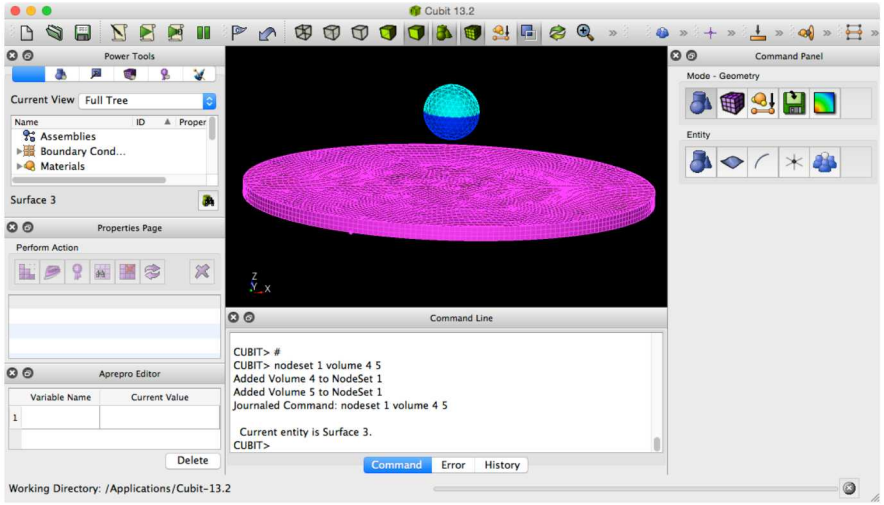

Peridigm Output

- Genesis file

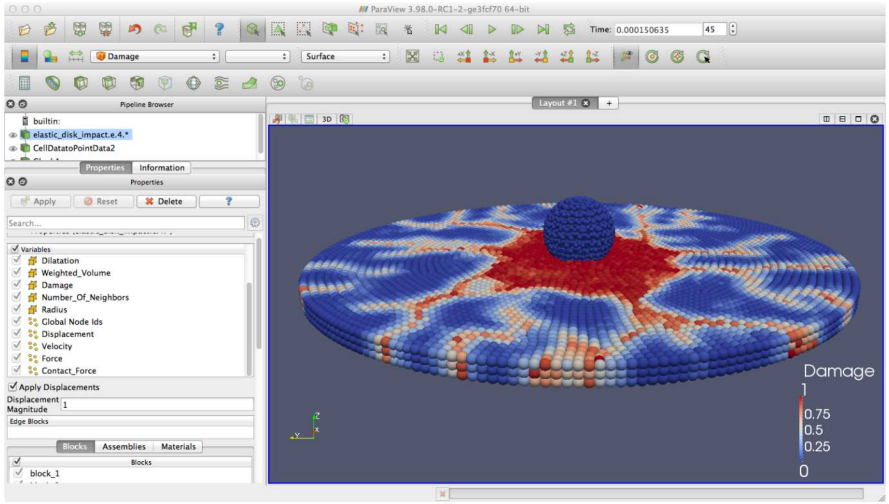

Simulation of a standard displacement-controlled tensile test

- Meshless discretization created from genesis hexahedral mesh (Cubit)
- Elastic correspondence model (classic stress-strain model)
- Prescribed displacement boundary conditions
- Quasi-static time integration
  - Newton solver
  - Construction of tangent stiffness matrix
- Compute classes for computing engineering stress and strain
  - Track ends of virtual strain gauge
  - Compute net reaction forces

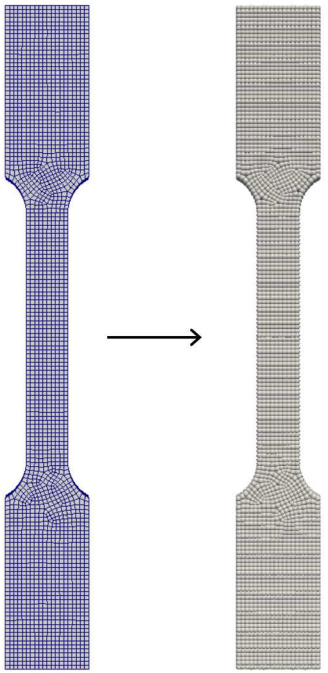

Discretization created by converting a hexahedral mesh to nodal volumes

Input deck (1 of 4)

```
Discretization
    Type "Exodus"
    Input Mesh File "tensile_test.g"

Materials
    My Material
      Material Model "Elastic Correspondence"
      Density 8.0
      Bulk Modulus 1.500e12
      Shear Modulus 6.923e11
      Hourglass Coefficient 0.02

Blocks
    My Block
      Block Names "block_1 block_2 block_3"
      Material "My Material"
      Horizon 0.16

Solver
    Initial Time 0.0
    Final Time 1.0
    QuasiStatic
      Number of Load Steps 4
      Absolute Tolerance 1.0
      Maximum Solver Iterations 10
```

Input deck (2 of 4)

```
Boundary Conditions
    Prescribed Displacement Bottom
      Type "Prescribed Displacement"
      Node Set "nodelist_1"
      Coordinate "y"
      Value "y*0.005*t"
    Prescribed Displacement Top
      Type "Prescribed Displacement"
      Node Set "nodelist_2"
      Coordinate "y"
      Value "y*0.005*t"
    Prescribed Displacement Fix Bottom Rigid Body Motion In X
      Type "Prescribed Displacement"
      Node Set "nodelist_3"
      Coordinate "x"
      Value "0.0"
    Prescribed Displacement Fix Bottom Rigid Body Motion In Z
      Type "Prescribed Displacement"
      Node Set "nodelist_4"
      Coordinate "z"
      Value "0.0"
    Prescribed Displacement Fix Top Rigid Body Motion In X
      Type "Prescribed Displacement"
      Node Set "nodelist_5"
      Coordinate "x"
      Value "0.0"
    Prescribed Displacement Fix Top Rigid Body Motion In Z
      Type "Prescribed Displacement"
      Node Set "nodelist_6"
      Coordinate "z"
      Value "0.0"
```

Input deck (3 of 4)

```
Compute Class Parameters
    Strain Gage Top Initial Position
      Compute Class "Nearest_Point_Data"
      X 0.0317
      Y 1.238
      Z 0.0
      Variable "Model_Coordinates"
      Output Label "Gage_Top_Initial_Position"
      Verbose "True"
    Strain Gage Bottom Initial Position
      Compute Class "Nearest_Point_Data"
      X 0.0317
      Y -1.238
      Z 0.0
      Variable "Model_Coordinates"
      Output Label "Gage_Bottom_Initial_Position"
      Verbose "True"
    Strain Gage Top Displacement
      Compute Class "Nearest_Point_Data"
      X 0.0317
      Y 1.238
      Z 0.0
      Variable "Displacement"
      Output Label "Gage_Top_Displacement"
      Verbose "True"
Strain Gage Bottom Displacement
      Compute Class "Nearest_Point_Data"
      X 0.0317
      Y -1.238
      Z 0.0
      Variable "Displacement"
      Output Label "Gage_Bottom_Displacement"
      Verbose "True
Top Reaction Force
      Compute Class "Block_Data"
      Calculation Type "Sum"
      Block "block_3"
      Variable "Force"
      Output Label "Top_Reaction_Force"
   Bottom Reaction Force
      Compute Class "Block_Data"
      Calculation Type "Sum"
      Block "block_1"
      Variable "Force"
      Output Label "Bottom_Reaction_Force"
```

Input deck (4 of 4)

```
Output
    Output File Type "ExodusII"
    Output Filename "tensile_test"
    Output Frequency 1
    Output Variables
      Displacement "true"
      Velocity "true"
      Element_Id "true"
      Proc_Num "true"
      Force_Density "true"
      Hourglass_Force_Density "true"
      Force "true"
      Volume "true"
      Gage_Top_Initial_Position "true"
      Gage_Bottom_Initial_Position "true"
      Gage_Top_Displacement "true"
      Gage_Bottom_Displacement "true"
      Top_Reaction_Force "true"
      Bottom_Reaction_Force "true"
      Deformation_Gradient "true"
      Cauchy_Stress "true"
      Radius "true"
      Number_Of_Neighbors "true"
      Neighborhood_Volume "true"
```

Output (1 of 3)

```
-- Peridigm
-- version 1.5.0 (Dev)

MPI initialized on 8 processors.

Nearest Point Data Compute Class:
  Requested variable: Model_Coordinates
  Requested location: 0.0317, 1.238, 0
  Closest Element Id: 6715
  Closest Element Position: 0.0317576, 1.23833, 8.35356e-17

Nearest Point Data Compute Class:
  Requested variable: Model_Coordinates
  Requested location: 0.0317, -1.238, 0
  Closest Element Id: 6676
  Closest Element Position: 0.0317605, -1.23854, 8.38424e-17

Nearest Point Data Compute Class:
  Requested variable: Displacement
  Requested location: 0.0317, 1.238, 0
  Closest Element Id: 6715
  Closest Element Position: 0.0317576, 1.23833, 8.35356e-17

Nearest Point Data Compute Class:
  Requested variable: Displacement
  Requested location: 0.0317, -1.238, 0
  Closest Element Id: 6676
  Closest Element Position: 0.0317605, -1.23854, 8.38424e-17

Allocating global tangent matrix...
  number of rows = 37875
  number of nonzeros = 30378033
```

Output (2 of 3)

```
Load step 1, initial time = 0, final time = 0.25, convergence criterion = 1
  iteration 1: residual = 6.15e+09
  iteration 2: residual = 1.46418e+08
  iteration 3: residual = 326680
  iteration 4: residual = 42.3547
  iteration 5: residual = 0.00403217
  cpu time for load step = 1.2e+02 sec., cumulative cpu time = 1.2e+02 sec.

Load step 2, initial time = 0.25, final time = 0.5, convergence criterion = 1
  iteration 1: residual = 6.1e+09
  iteration 2: residual = 1.4e+06
  iteration 3: residual = 2.8e+02
  iteration 4: residual = 0.042
  cpu time for load step = 65 sec., cumulative cpu time = 1.9e+02 sec.

Load step 3, initial time = 0.5, final time = 0.75, convergence criterion = 1
  iteration 1: residual = 6.1e+09
  iteration 2: residual = 1.4e+06
  iteration 3: residual = 2.3e+02
  iteration 4: residual = 0.035
  cpu time for load step = 64 sec., cumulative cpu time = 2.5e+02 sec.

Load step 4, initial time = 0.75, final time = 1, convergence criterion = 1
  iteration 1: residual = 6.1e+09
  iteration 2: residual = 1.4e+06
  iteration 3: residual = 1.9e+02
  iteration 4: residual = 0.029
  cpu time for load step = 63 sec., cumulative cpu time = 3.1e+02 sec.
```

Output (3 of 3)

```
Memory Usage (Heap Alloc MB):
                                    Min           Max           Ave
  Zoltan Search Tree                 12            12            12
  Post Execute                       70            88            79
  Allocated Jacobian            1.2e+02       1.4e+02       1.3e+02

Wallclock Time (seconds):
                                    Min           Max           Ave
  Total                         3.2e+02       3.2e+02       3.2e+02
  Solve Linear System           1.7e+02       1.7e+02       1.7e+02
  Output                          0.086          0.14          0.12
  Line Search                       2.5           2.5           2.5
  Internal Force                    1.8           1.9           1.8
  Gather/Scatter                      1           1.1           1.1
  Evaluate Jacobian             1.4e+02       1.4e+02       1.4e+02
  Compute Residual                  2.8           2.9           2.9
  Apply Kinematic B.C.           0.0011         0.016        0.0044
  Apply Initial Conditions            0       1.2e-06       5.1e-07
  Apply Boundary Conditions        0.17           6.9           1.8
  Apply Body Forces             1.5e-05       3.4e-05       1.9e-05
  Allocate Global Tangent             7             7             7
```

Results

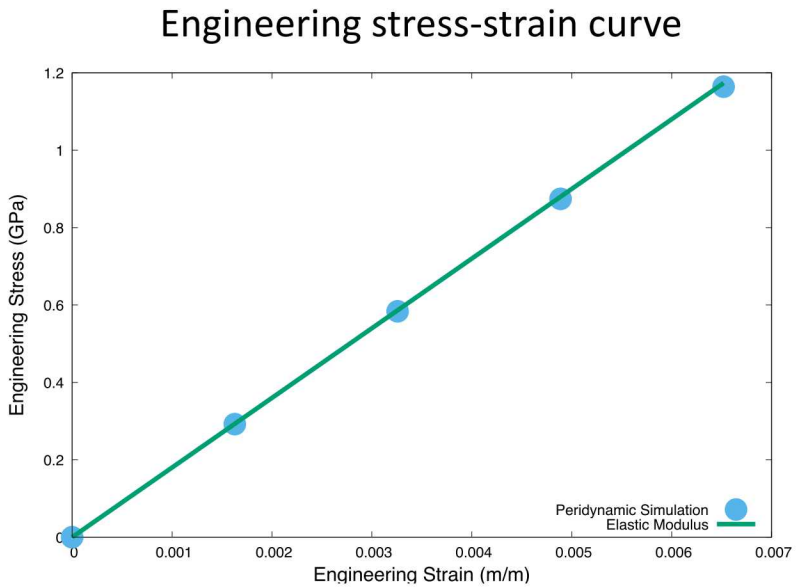
Engineering stress-strain curve
Engineering Stress (GPa)
Engineering Strain (m/m)
1.2
1
0.8
0.6
0.4
0.2
0
0.001
0.002
0.003
0.004
0.005
0.006
0.007
Peridynamic Simulation
Elastic Modulus

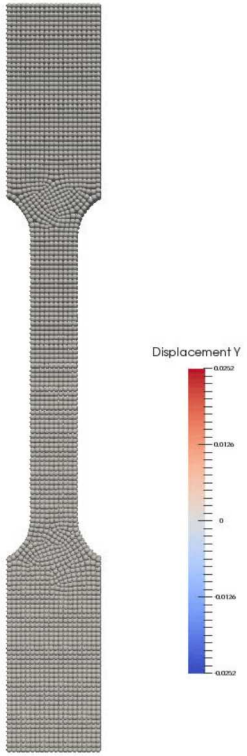
Displacement Y

Simulation of impact / brittle fracture

- Meshless discretization created from genesis hex/tet mesh (Cubit)
- Linear Peridynamic Solid material model
- Critical stretch bond failure rule applied to target
- Multiple material blocks (projectile, target)
- Explicit transient dynamics
- Short-range force contact model
- Initial velocity applied to projectile
- Standard exodus output, plus history output for global data

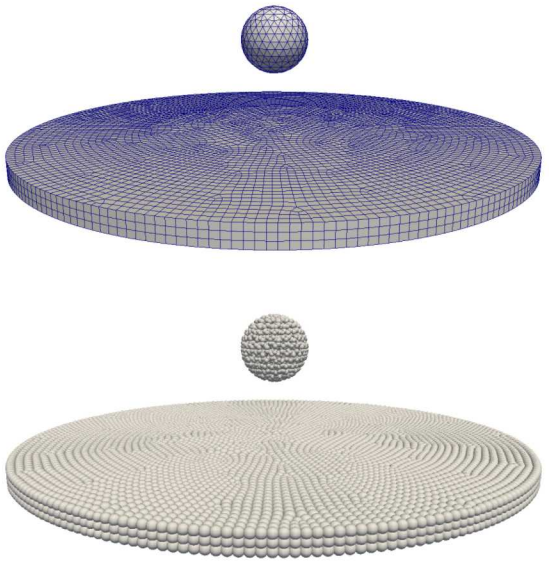

Discretization created by converting a hex/tet mesh to nodal volumes

Input deck (1 of 4)

```
Discretization
    Type "Exodus"
    Input Mesh File "disk_impact.g"

Materials
    Disk Material
        Material Model "Elastic"
        Density 2200.0
        Bulk Modulus 14.90e9
        Shear Modulus 8.94e9
    Ball Material
        Material Model "Elastic"
        Density 7700.0
        Bulk Modulus 160.00e9
        Shear Modulus 78.30e9

Damage Models
    Disk Damage Model
        Damage Model "Critical Stretch"
        Critical Stretch 0.0005
```

Input deck (2 of 4)

```
Blocks
    Disk Block
        Block Names "block_1”
        Material "Disk Material”
        Damage Model "Disk Damage Model”
        Horizon 0.0031
    Ball Block
        Block Names "block_2”
        Material "Ball Material”
        Horizon 0.0031

Contact
    Search Radius 0.01
    Search Frequency 100
    Models
        My Contact Model
            Contact Model "Short Range Force”
            Contact Radius 0.000775
            Spring Constant 1.0e12
    Interactions
        Interaction Disk with Ball
            First Block "block_1"
           Second Block "block_2”
            Contact Model "My Contact Model"
```

Input deck (3 of 4)

```
Boundary Conditions
    Sphere Initial Velocity
        Type "Initial Velocity”
        Node Set "nodelist_1”
        Coordinate "z”
        Value "-100.0”

Solver
    Initial Time 0.0
    Final Time 0.0008
    Verlet
        Safety Factor 0.7
```

Input deck (4 of 4)

```
# Output file for full data set, disk_impact.e
Output_1
    Output File Type "ExodusII"
    Output Filename "disk_impact"
    Output Frequency 350
    Output Variables
        Displacement "true"
        Velocity "true"
        Element_Id "true"
        Proc_Num "true"
        Dilatation "true"
        Weighted_Volume "true"
        Force "true"
        Contact_Force "true"
        Damage "true"
        Number_Of_Neighbors "true"
        Radius "true"

# Output file for history data (global data), disk_impact.h
Output_2
    Output File Type "ExodusII"
    Output Filename "disk_impact"
    Output Frequency 35
    Output Variables
        Global_Kinetic_Energy "true"
        Global_Linear_Momentum "true"
        Global_Angular_Momentum "true"
```

Output

```
-- Peridigm
-- version 1.5.0 (Dev)

MPI initialized on 8 processors.

** Warning: the selected contact search radius, 0.01, is large
** relative to the maximum element diameter (0.000735518).
** This may lead to the memory capacity being exceeded.

Time step (seconds):
  Stable time step    1.59402e-07
  User time step      not provided
  Safety factor       0.7
  Time step           1.11581e-07

Total number of time steps 7169

Explicit time integration [==================100% Complete]

Memory Usage (Heap Alloc MB):
                                    Min           Max           Ave
  Zoltan Search Tree              73.8654       117.254       95.4224
  Post Execute                    38.5572       63.4641       50.5217
  Contact Initialized             17.7726       26.7634       21.5481

Wallclock Time (seconds):
                                    Min           Max           Ave
  Total                           6.4e+02       6.4e+02       6.4e+02
  Rebalance                       1.8e+02       1.8e+02       1.8e+02
  Output                               16            17            17
  Internal Force                  2.1e+02       3.8e+02       2.9e+02
  Initialize Contact Maps         0.00083        0.0022        0.0014
  Gather/Scatter                       64       2.4e+02       1.5e+02
  Apply Kinematic B.C.             0.0051         0.011        0.0078
  Apply Initial Conditions         3.9e-05        0.0012       0.00052
  Apply Body Forces                  0.047         0.078         0.062
```

Results

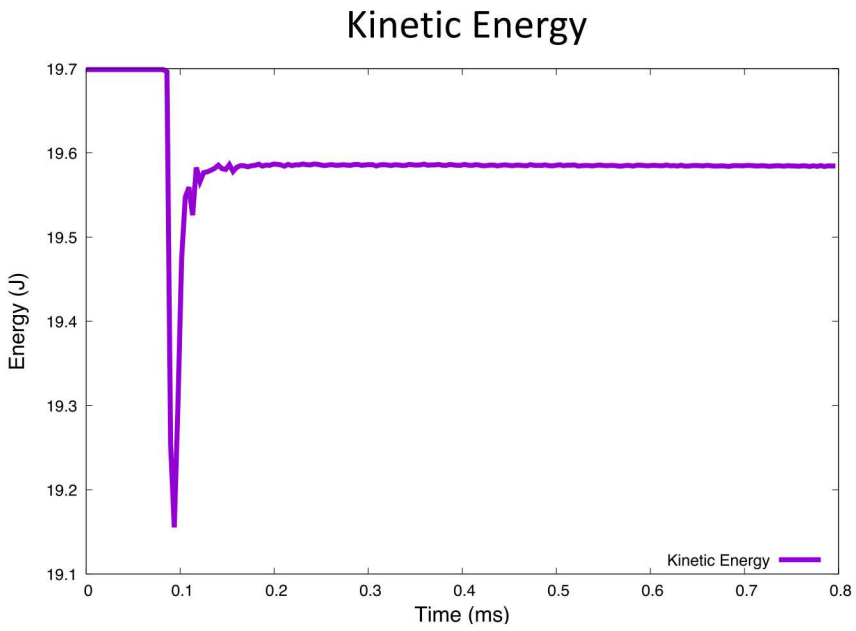
Kinetic Energy
Energy (J)
19.7
19.6
19.5
19.4
19.3
19.2
19.1
0
0.1
0.2
0.3
0.4
0.5
0.6
0.7
0.8
Time (ms)
Kinetic Energy

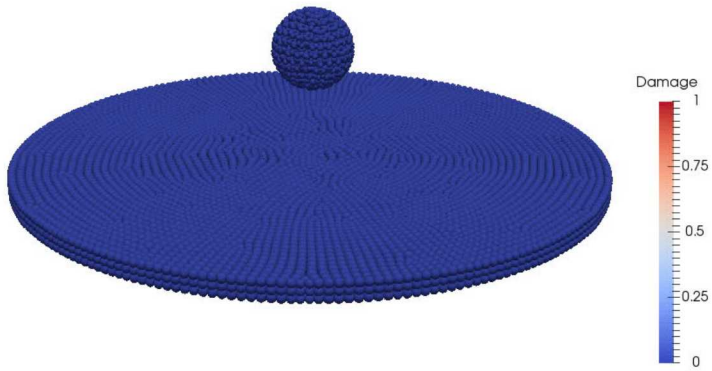
Damage
1
0.75
0.5
0.25
0

Hands-on Examples